Bioorganic Chemistry 92 (2019) 103262

Contents lists available at ScienceDirect

Bioorganic Chemistry

journal homepage: www.elsevier.com/locate/bioorg

First example of Azo-Sulfa conjugated chromene moieties: Synthesis, characterization, antimicrobial assessment, docking simulation as potent class I histone deacetylase inhibitors and antitumor agents

Rawda M. Okasha[a], Mosa Alsehli[a], Saleh Ihmaid[b], Sultan S. Althagfan[c], Mohamed S.A. El-Gaby[d], Hany E.A. Ahmed[b,e], Tarek H. Afifi[a,f,*]

[a] Chemistry Department, Faculty of Science, Taibah University, 30002, Al-Madinah Al-Munawarah, Saudi Arabia
[b] Pharmacognosy and Pharmaceutical Chemistry Department, Pharmacy College, Taibah University, Al-Madinah Al-Munawarah, Saudi Arabia
[c] Clinical and Hospital Pharmacy Department, Taibah University, College of Pharmacy, Taibah University, Al-Madinah Al-Munawarah 41477, Saudi Arabia
[d] Department of Chemistry, Faculty of Science, Al-Azhar University at Assiut, Assiut 71524, Egypt
[e] Pharmaceutical Organic Chemistry Department, Faculty of Pharmacy, Al-Azhar University, 11884 Nasr City, Cairo, Egypt
[f] Chemistry Department, Faculty of Science, Al-Azhar University, 11884 Nasr City, Cairo, Egypt

ARTICLE INFO

Keywords:
Chromene
Sulfonamide
Antimicrobial
Anticancer activity
HDAC examination

ABSTRACT

This report presents the development of a novel and primary model of sulfonamide compounds encompassing a chromene azo motif with the intent of becoming applicable for drug candidates in the cases of drug-resistant pathogens. The novel molecules (**7a–n**) have been synthesized via a two-step reaction. First, 4-((2, 4-dihydroxyphenyl)diazenyl)benzenesulfonamide (**3a–e**) were obtained through the reaction of their corresponding diazotized 4-aminobenzenesulfonamides (**1a–e**) with resorcinol, followed by the heterocyclization of **3a–e** with arylidenemalononitriles (**6a–d**). Upon structural identification, the newly synthesized compounds were evaluated for their antibacterial and antifungal activities. Moreover, their cytotoxic screening was performed against three cancer cell lines: HCT-116, HepG-2, and MCF-7. Further examinations were comprised of the inhibitory effect analyses of the novel sulfonamide/chromene derivatives against the HDAC classes and the Tubulin polymerization in order to discern the prime antitumor drug candidates.

1. Introduction

Drug resistance is a decisive threat to global public health and represents a challenge to a wide range of disciplines, including; resistance mechanisms, infection control, virulence genes, and drug design [1,2]. Two of the most common prevalent cases of drug resistance are in the antimicrobial and antitumor pathogens. The development of antimicrobial resistance has become a major problem in healthcare, which arises mainly from the overuse and misuse of antibiotics that enhances the manipulative properties of bacteria. In general, the deceptive mechanism of bacteria could be achieved through the neutralization of the antibiotic or the alteration of their outer structure that prevents the antibiotic's abilities. Therefore, the treatment of infections provides more obstacles as bacteria continues to evolve and as a lack of progress in developing new antibiotics persists [1,2].

Additionally, in the cancer diagnoses research, drug resistance is one of the greatest difficulties that causes failure in tumor treatment, a recurrence of the disease, or even the death of a patient. Resistance to drugs can be present during diagnosis or it can develop after the treatment of the tumor. However, the development of new medication continues to offer hope to prohibit the resistance capabilities of the tumor cell lines [3–5].

Recently, the development of new materials with interesting biological activities is a major target to overcome the resistance toward the present drugs. Chromene molecules are one of the most demanded compounds that are recognized as one type of 'privileged medicinal scaffolds' due to their unique pharmacological and biological activities [6–13]. Derivatives of these molecules exhibit tremendous medicinal behaviors such as antimicrobial and antifungal [12,14–16], antiproliferation [9–11,13,17–19], antioxidant [6,20], antispasmolytic, estrogenic [21], antileishmanial [22], hypotensive [8], vascular-disrupting activity [23], and blood platelet antiaggregating effects [24]. In addition, these molecules have been used in the enhancement of cognitive functions for the treatment of neurodegenerative symptom [25],

* Corresponding author at: Chemistry Department, Faculty of Science, Taibah University, 30002, Al-Madinah Al-Munawarah, Saudi Arabia.
E-mail address: afifith@yahoo.com (T.H. Afifi).

https://doi.org/10.1016/j.bioorg.2019.103262
Received 3 July 2019; Received in revised form 2 September 2019; Accepted 5 September 2019
Available online 05 September 2019
0045-2068/ © 2019 Elsevier Inc. All rights reserved.

as well as treating Alzheimer's disease [26] and Schizophrenia disorder [27]. Moreover, the incorporation of a suitable heterocyclic moiety such as chromene derivatives with an azo linkage increases their medicinal performance for particular usage as antibacterial [28,29], antimicrobial [30,31], antioxidant [32], and other useful chemotherapeutic agents [33].

Additionally, molecules containing sulfonamide moieties, sulfa drugs, have been acknowledged for their remarkable medicinal and biological applications [34–41]. Moreover, researchers have extensively employed sulfa drugs in infection treatments, particularly for patients intolerant to antibiotics. The broad spectrum of the sulfonamide's activities against Gram-positive and Gram-negative bacteria arises from their capacity to hinder the production process of the folic acid in the bacterial cells, subsequently, triggering their death. The implementations of sulfonamide molecules encompass an assortment of assays, including: antibacterial, antifungal, antitumor agents, anticonvulsants and protease inhibitors, carbonic anhydrase inhibitors, diuretics, hypoglycemic agents, thyroid inhibitors, and HDAC inhibitors [34–41]. In this report, our foremost passion is to create a new class of drug-like candidates, established from the merging of the 4*H*-chromene, azo, and sulfonamide moieties as proposed in Fig. 1. The aforesaid design was propositioned for synthesis due to the beneficial facets as anticancer agents, resulting from the sulphonamide functionality as a privileged motif binding to the HDAC target. The antimicrobial and cytotoxicity effects of these novel materials have been exploited as well as their *in vitro* HDACs inhibitory activity.

2. Results and discussions

2.1. Chemistry

2.1.1. Synthesis and characterization

It is established that the high reactivity of resorcinol is primarily associated with the location of these two hydroxyl groups in the benzene ring. As far as the reactivity of resorcinol is concerned, the hydrogen atoms adjacent to the hydroxyl groups, namely at carbon atoms 2, 4, and 6, are particularly reactive. The hydrogen atom located at the 5-position of the resorcinol molecule is basically non-reactive and,

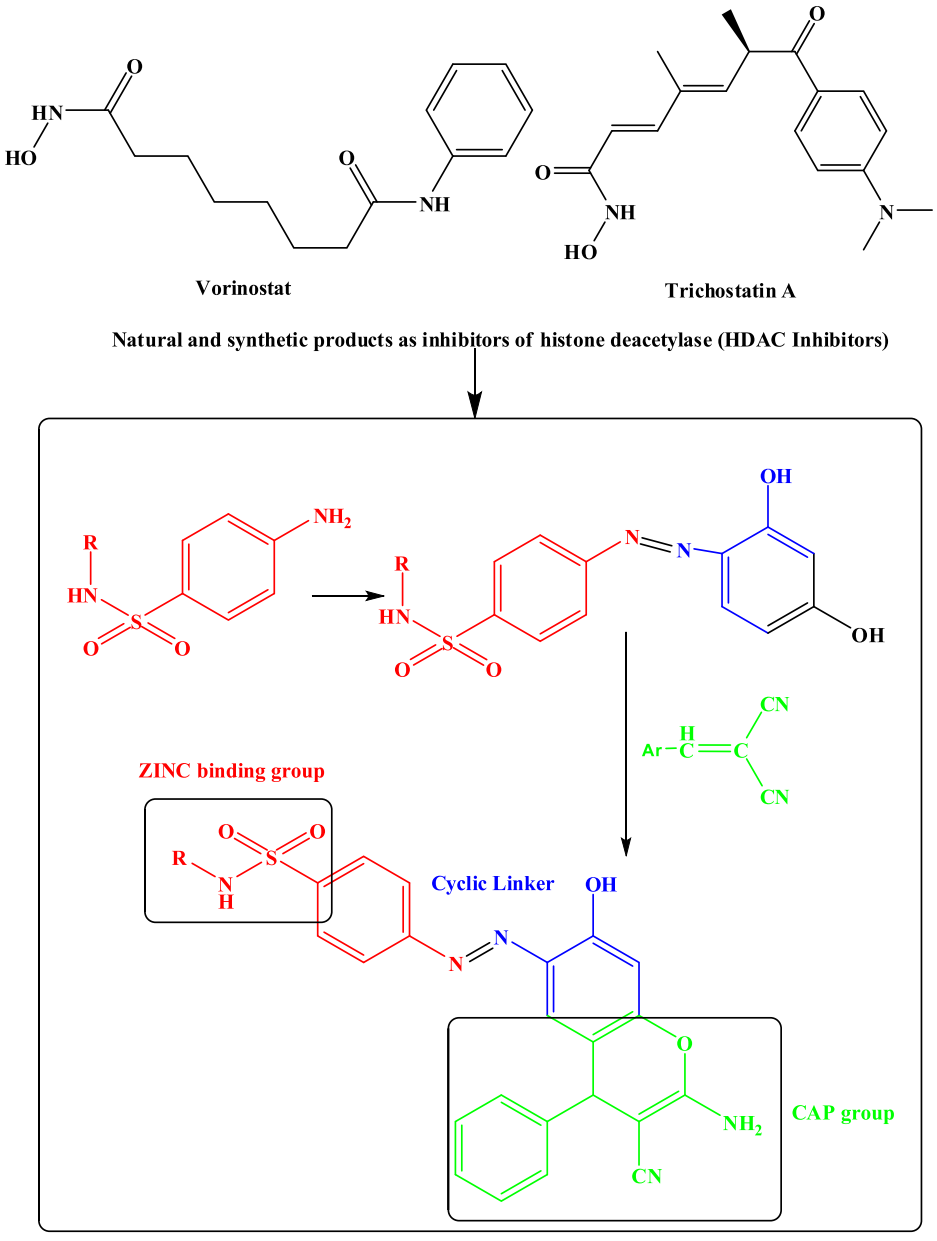

Fig. 1. The design of novel chromene linked to sulfonamide moiety.

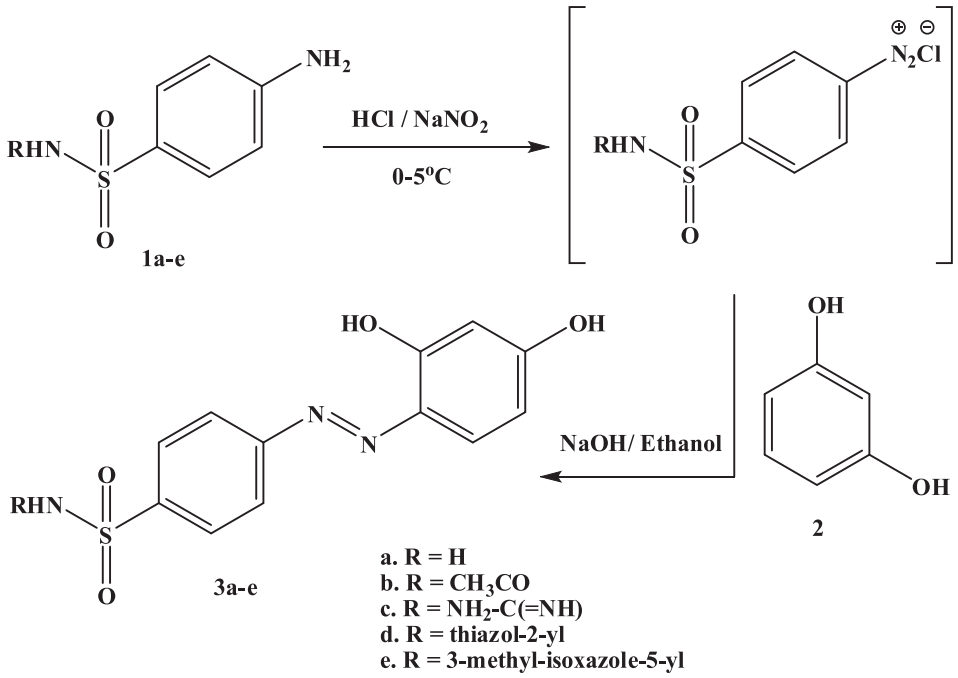

Scheme 1. Synthesis of 4-((2, 4-dihydroxyphenyl)diazenyl)benzenesulfonamide **3a–e.**

therefore, does not take part in any chemical reactions under normal reaction conditions [42]. A series of 4-((2, 4-dihydroxyphenyl)diazenyl) benzenesulfonamide (**3a–e**) were synthesized in good yields by the coupling of diazotized 4-aminobenzenesulfonamides (**1a–e**) with resorcinol in the presence of 10% sodium hydroxide. The diazotization was carried out in the presence of nitrosyl chloride at 0–5 °C, Scheme 1.

The structures of the synthesized compounds **3a–e** were established on the basis of their analytical and spectral data. The infrared spectra of compounds **3a–e** displayed absorption band at 1597–1627 cm^{-1}, which is a characteristic of the azo group (N=N) in addition to the absorption of the hydroxyl, amino, imino, and sulfone moieties. The representative ^{1}H NMR spectrum of compound **3a** (DMSO-d_6) presented singlet signals at δ 7.45 and 12.19 ppm, assigned to the NH_2 and OH protons, respectively, which is exchangeable with the D_2O. A pair of doublets at δ 6.54 and 7.69 ppm and a singlet at 6.38 ppm was assigned to the aromatic protons of the phenolic ring with the broad singlet at δ 8.03 ppm attributable to the aromatic protons of the benzene sulfonamide. The mass spectrum of compound **3d** revealed a molecular ion peak at *m/z* 376 (2.76%), corresponding to the molecular formula $C_{15}H_{12}N_4O_4S_2$. The base peak was discovered to be at *m/z* 92 (100%), which is a characteristic of the C_6H_5NH moiety.

The reactivity of the nucleaphilic molecules, 4-((2, 4-dihydroxyphenyl)diazenyl)benzenesulfonamide (**3a–e**), towards the electrophilic arylidenemalononitriles (**6a–d**) was investigated. The reaction of compounds **3a–e** with benzaldehyde derivatives (**4a–d)** and Malononitrile (**5)** in ethanol at a reflux temperature in the presence of a catalytic amount of piperidine furnished the respective 4-((2-amino-3-cyano-4-aryl-7-hydroxy-4-aryl-4*H*-chromen-6-yl)diazenyl] benzenesulfonamides (**7a–n**) in quantitative yields, Scheme 2.

The structure of the chromene derivative **7a**, as a representative example, was established based on the foundation of its spectral data. The IR spectra showed the stretching vibration bands at 3439, 2190, and 1589 cm^{-1} for (OH), (CN), and (N=N), respectively. Furthermore, the (NH_2) group divulged a resonance of a pair of bands at 3357 and 3203 cm^{-1}. The ^{1}H NMR exhibited singlet signals at δ 4.77 and 12.01 ppm for the CH-pyran at the 4-position and the (OH) group, respectively [12]. Moreover, a broad signal at δ 7.05 ppm was attributed to the amino protons while the multiple signals at δ 6.80, 7.12–7.20, 7.22–7.33, and 7.76 ppm was attributed to the aromatic protons of the phenyl group at the 4-position in the pyran ring, while, the two doublets at δ 8.02 & 8.14 ppm to the aromatic sulfonamide protons. Additionally, the ^{13}C NMR spectra revealed a characteristic signal at δ 28.51 ppm, which corresponds to the C-4 of the pyran ring [12].

A plausible mechanism for the formation of the novel chromene derivatives **7a–n** was illustrated in Scheme 3. The proposed strategy produces the suggestion that the deprotonation of the 4-((2, 4-dihydroxyphenyl)diazenyl)benzenesulfonamide (**3a–e**) with piperidine generated the aniones **4a–e** that can, subsequently, perform the Michael addition with the arylidenemalononitriles **5a–d** to give the non-isolable Michael adducts **6a–m**, which underwent spontaneous cyclization to afford the chromene skeletons **7a–n**.

2.1.2. UV–vis study

The UV–visible study of the sulfa containing azo chromophores **3a–e** and their chromene counterparts' 7a-n was performed in a DMF solvent in order to discover their wavelength maximum (λ_{max}) values. The obtained data, as presented in Table 1, revealed that the formation of the chromene azo sulfa derivatives, in majority of cases, did not alter the λ_{max} values of their azo precursors due to the non-conjugated system of the chromene sulfa moieties. All the sulfa azo chromophores and their chromene analogues portrayed λ_{max} values in the range of 387–445 nm.

2.2. Biological screening

2.2.1. Antimicrobial screening

All the newly synthesized compounds (**3a–e**) and (**7a–n**) and their precursors (**1a–e**) were screened for their antibacterial, antifungal, and antimycobacterium activities via the agar diffusion well method [35] while the inhibition zones and the minimum inhibitory concentrations (MIC) were determined by the serial dilution method [36]. It is imperative to cite that the microbial activities of compounds **1** and **3** have been evaluated in order to derive a comparison between the activity of the chromene molecules containing azo sulfonamide and their precursor, which consequently clarify the role of the chromene moieties in this class of activity. The activity of the synthesized compounds was tested against four Gram-positive bacteria, including *Streptococcus pneumoniae* (RCMB 010010), *Bacillus subtilis*(RCMB 010067),

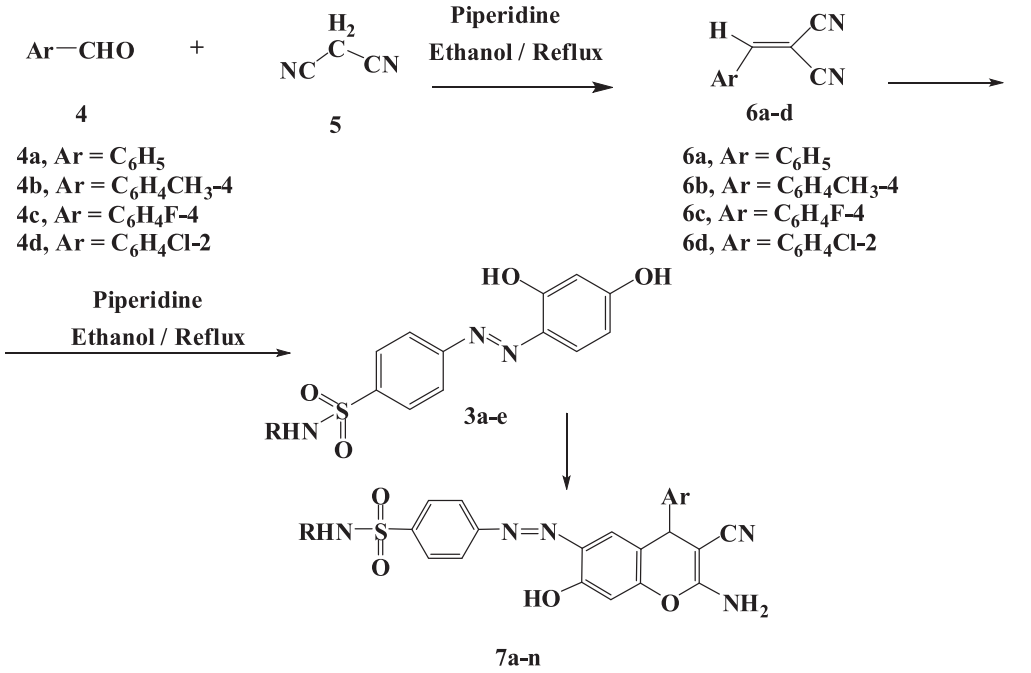

7a; R = H, Ar = C_6H_5
7b; R = H, Ar = C_6H_4F-4
7c; R = $COCH_3$, Ar = $C_6H_4CH_3$-4
7d; R = $COCH_3$, Ar = C_6H_4F-4
7e; R = $COCH_3$, Ar = C_6H_4Cl-2
7f; R = NH_2-C(=NH), Ar = C_6H_5
7g; R = NH_2-C(=NH), Ar = C_6H_4Cl-2
7h; R = NH_2-C(=NH), Ar = C_6H_4F-4
7i; R = thiazol-2-yl, Ar = $C_6H_4CH_3$-4
7j; R = thiazol-2-yl, Ar = C_6H_4F-4
7k; R = thiazol-2-yl, Ar = C_6H_4Cl-2
7l; R = 3-methylisoxazol-5-yl, Ar = $C_6H_4CH_3$-4
7m; R = 3-methylisoxazol-5-yl, Ar = C_6H_4F-4
7n; R = 3-methylisoxazol-5-yl, Ar = C_6H_4Cl-2

Scheme 2. Synthesis of chromene derivatives **7a–n.**

Staphylococcus aureus (RCMB 000106), and *Methicillin-Resistant Staphylococcus aureus* (MRSA 2658 RCMB); three Gram-negative bacteria, including *Pseudomonas aeruginosa* (RCMB 010043), *Escherichia coli* (RCMB 010052), and *Salmonella typhimurium* (RCMB 000106); and four fungi, including *Aspergillus fumigatus* (RCMB 02568), *Syncephalastrumracemosum* (RCMB 05922*), Geotricumcandidum* (RCMB 05097), and *Candida albicans* (RCMB 05036), with a *Mycobacterium tuberculosis* strain (RCMB 010094-8). Ampicillin, Ciprofloxacin, Amphotericin B, and Vancomycin were exploited as control drugs. The observed antimicrobial data of the target compounds and the reference drugs: the inhibition zone (IZ) and the minimum inhibitory concentrations (MIC) are given in Tables 2 and 3 and presented in Figs. 2 and 3. The data

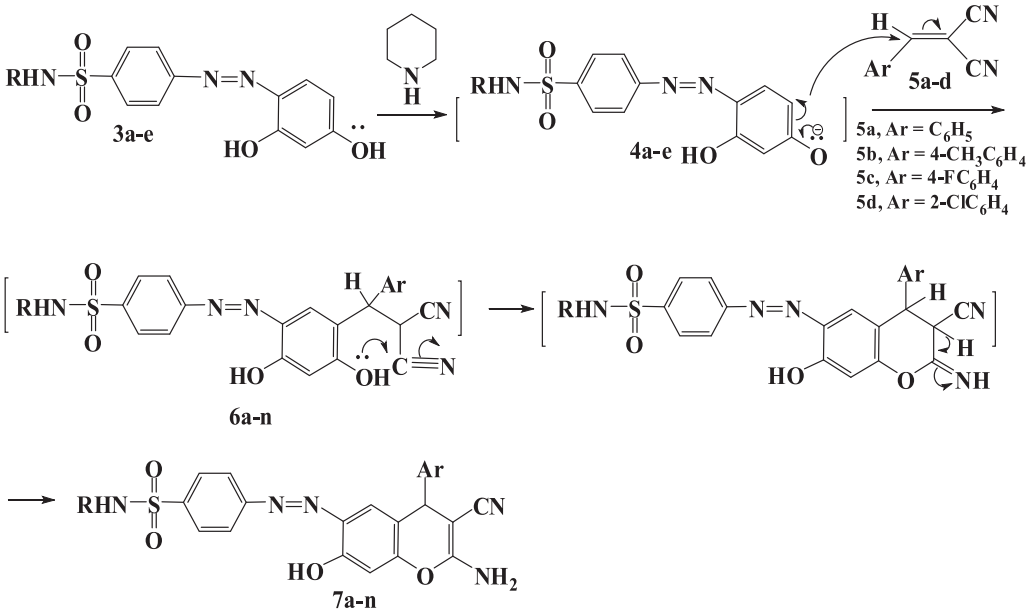

Scheme 3. Proposed mechanism for the formation of Chromene derivaties **7a–n.**

Table 1
UV–vis study of the new azosulfonamide bearing chromenes 7a-n and their precursors **3a–e**.

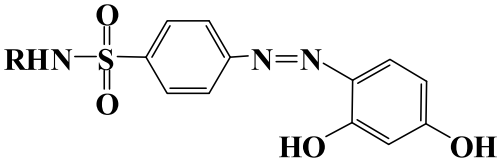

3a-e

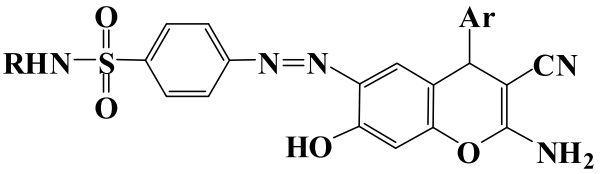

7a-n

Compound	R	Ar	λ_{max} (nm)
3a	H——		396
7a	H——	C_6H_5	395
7b	H——	C_6H_4F-4	398
3b	$H_3C-\overset{O}{\overset{\|}{C}}-$		400
7c	$H_3C-\overset{O}{\overset{\|}{C}}-$	$C_6H_4CH_3$-4	398
7d	$H_3C-\overset{O}{\overset{\|}{C}}-$	C_6H_4F-4	390
7e	$H_3C-\overset{O}{\overset{\|}{C}}-$	C_6H_4Cl-2	397
3c	$H_2N-\overset{NH}{\overset{\|}{C}}-$		400
7f	$H_2N-\overset{NH}{\overset{\|}{C}}-$	C_6H_5	394
7g	$H_2N-\overset{NH}{\overset{\|}{C}}-$	C_6H_4F-4	387
7h	$H_2N-\overset{NH}{\overset{\|}{C}}-$	C_6H_4Cl-2	388
3d	**thiazol-2-yl**		398
7i	**thiazol-2-yl**	$C_6H_4CH_3$-4	390
7j	**thiazol-2-yl**	C_6H_4F-4	392
7k	**thiazol-2-yl**	C_6H_4Cl-2	392
3e	**3-methyl-isoxazol-5-yl**		401
7l	**3-methyl-isoxazol-5-yl**	$C_6H_4CH_3$-4	445
7m	**3-methyl-isoxazol-5-yl**	C_6H_4F-4	398
7n	**3-methyl-isoxazol-5-yl**	C_6H_4Cl-2	396

disclosed that most of the tested compounds exhibited appreciable bacterial and fungal inhibition in comparison to the reference drugs. In general, the synthesized compounds were more active against the Gram-negative bacteria, displaying an IZ value of more than 20. Among the synthesized compounds, **7e–j** were found to be more effective against *E. coli*, with the IZ values ranging from 21 to 24 mm and the MIC values from 0.49 to 3.9 μg/ml. Meanwhile, compounds **7e– g** and **7j** were discovered to be more active against *S.T* with IZ values of 22–26 mm. In the case of the antibacterial activity against the Gram-positive bacteria, most of the novel compounds were found to be comparable in activity to the reference drugs, MIC ranging from 3.9 to 0.49 μg/mL. In particular, **7 g** exhibited mild inhibitory activity towards MRSA, IZ = 21.3 mm and MIC = 3.9 μg/mL. Through in-depth analyses of the novel derivatives, it was detected that the aromatic substituents possessed an impact on the inhibitory activities of the synthesized chromene azosulfonamide derivatives. For instance, the most potent antimicrobial compounds **7e–g** had a 2-chloro substituent with terminal amino or acetyl groups, which assures the incidence of broad activity against a wild bacterial range. Additionally, the combination of the halogen substituent with the heterocyclic aromatic systems of 3-methylisoxazolyl stemmed an accepted range of their antimicrobial effects. Overall, the chromene fragments with the different aryl or heteroaryl substituents revealed significant antimicrobial behavior. Moreover, the desired compounds were moderately or slightly more active against the examined fungal species. Thus, our investigation of the antimicrobial activity of the novel derivatives displayed more potency than the reference drugs against the Gram-negative bacteria and mild activity towards the Gram positive, fungi, and the mycobacterium strain.

2.2.2. Cytotoxic screening

The *in vitro* cytotoxic activity was performed, utilizing the MTT assay [39] against three human carcinoma cell lines: human colon carcinoma (HCT-116), human hepatocellular carcinoma (HepG-2), human breast adenocarcinoma (MCF-7) cell lines. Doxorubicin was used as a positive control, which has high cytotoxicity. The inhibitory effects of compounds **1a–e**, **3a–e**, and **7a–n** on the growth of the three cell lines are described in Table 4 and Fig. 4. As mentioned previously, the cytotoxic activities of compounds **1** and **3** have been appraised in order to derive a comparison between the activity of the chromene molecules containing azo sulfonamide and their precursors, which consequently elucidate the performance of the chromene moieties in this class of activity. The sulfa compound class **1a–e** exhibited less potency as cell growth inhibitors. As anticipated, the inhibitory behavior was increased by the 10-fold effect via the incorporation of the azo moieties in compounds **3a–e**. Moreover, the combination of the chromene motifs into these derivatives enhanced the potent cytotoxicity when evaluated against the reference drugs. Within the evaluation of the azo/chromene-based sulfa molecules, it was discerned that the 4-aryl substituents demonstrate more activity than their 2-postioned analogues and the non-substituted rings. Hence, the 4-fluro divulged the highest potent antiproliferative effect linked to the azo derivatives of the sulfaisoxazole moiety, followed by the 4-methyl derivative of the chromene compounds of the sulfacetamide structure, Fig. 4.

The cytotoxic effects of compounds on colon, breast, and liver cell lines, following the exposure to different concentrations of the target

Table 2
Antimicrobial activity of the synthetic compounds (Inhibition Zone, IZ, diameter (mm)) (1 mg/mL in DMSO).

Compounds	Gm + ve			Gm-ve				Fungi			
	S.P	B.S	S.A	MRSA	P.A	E.C	S.T	A.F	S.R	G.C	C.A
1a	NA	16.3	18.2	NA	NA	17.8	18.9	15.2	17.3	19.3	NA
1b	20.4	26.8	19.2	19.2	17.6	21.6	24.3	22.4	NA	24.3	19.3
1c	17.1	19.3	16.2	NA	NA	18.3	20.4	15.7	NA	18.1	14.2
1d	18.6	20.1	17.2	NA	NA	16.4	19.8	13.2	12.3	15.6	NA
1e	18.3	22.3	16.1	NA	14.3	19.6	21.6	18.3	NA	20.2	14.3
3a	NA	22.3	25.6	NA	NA	21.8	22.9	21.3	23.2	24.4	NA
3b	21.6	23.4	20.6	21.2	NA	21.4	24.2	22.3	21.4	24.6	NA
3c	21.5	23.2	20.1	NA	NA	20.8	23.4	19.3	NA	21.6	20.8
3d	20.4	22.6	19.8	21.3	NA	19.3	21.8	21.3	20.8	21.6	NA
3e	19.3	21.3	23.3	14.6	NA	20.3	23.4	18.3	20.1	22.4	NA
7a	NA	20.1	21.3	NA	NA	19.4	21.2	16.3	18.4	19.9	NA
7b	NA	18.1	20.3	NA	NA	18.6	20.4	19.3	19.9	21.2	NA
7c	19.8	22.7	19.6	NA	NA	21.2	23.2	20.6	21.2	22.1	NA
7d	17.6	19.2	17.3	NA	NA	16.2	18.1	18.6	20.1	20.6	NA
7e	16.3	18.2	16.4	NA	NA	15.2	15.8	17.3	19.4	20.1	NA
7f	18.9	20.1	21.3	18.3	NA	19.1	20.9	17.2	NA	19.1	16.6
7g	18.3	19.6	18.4	NA	NA	18.9	20.5	16.3	NA	18.6	16.1
7h	22.3	23.9	20.8	20.1	NA	18.9	20.5	20.8	NA	22.3	21.8
7i	19.2	20.9	17.2	NA	NA	17.1	18.3	17.6	16.8	19.1	NA
7j	17.3	19.2	16.4	NA	NA	14.6	17.3	15.2	14.6	15.9	NA
7k	17.9	20.1	16.9	NA	NA	15.6	18.3	16.2	14.9	16.2	NA
7l	16.4	16.9	17.2	NA	NA	16.2	19.1	14.6	16.2	16.9	NA
7m	18.6	19.3	21.2	15.4	NA	19.3	21.6	17.6	19.2	21.1	NA
7n	20.4	21.7	23.8	18.4	NA	21.1	23.6	20.3	22.1	23.4	NA
Ampicillin	23.8	32.4	26.2	–	–	–	–	–	–	–	–
ciprofloxacin	–	–	–	–	17.3	19.9	22.3	–	–	–	–
Amphotericin B	–	–	–	–	–	–	–	23.7	19.7	28.7	25.4
Vancomycine	–	–	–	20.3	–	–	–	–	–	–	–

Mean zone of inhibition in mm from at least three experiments; (NA) means no activity.

Table 3
The antimicrobial activity of the synthetic compounds (Minimum inhibitory concentration, MIC, μg/mL).

Compounds	Gm + ve				Gm-ve			Fungi			
	S.P	B.S	S.A	MRSA	P.A	E.C	S.T	A.F	S.R	G.C	C.A
1b	3.9	0.49	3.9	3.9	15.63	1.95	0.49	0.98	NA	0.49	3.9
3a	NA	0.98	0.49	NA	NA	0.98	0.98	0.98	0.98	0.49	NA
3b	0.98	0.98	3.9	1.95	NA	1.95	0.49	0.98	1.95	0.49	NA
3c	1.95	0.98	3.9	NA	NA	1.95	0.98	3.9	NA	1.95	1.95
3d	3.9	0.98	3.9	1.95	NA	3.9	0.98	1.95	1.95	0.98	NA
3e	3.9	1.95	0.98	32.5	NA	3.9	0.98	7.81	3.9	0.98	NA
7b	NA	7.81	3.9	NA	NA	3.9	3.9	3.9	3.9	1.95	NA
7c	3.9	0.98	3.9	NA	NA	1.95	0.98	1.95	1.95	0.98	NA
7f	3.9	3.9	1.95	7.81	NA	3.9	1.95	15.63	NA	3.9	15.63
7g	0.98	0.49	1.95	3.9	NA	0.98	0.49	1.95	NA	0.98	0.98
7n	3.9	0.98	0.49	7.81	NA	1.95	0.49	3.9	0.98	0.98	NA
Ampicillin	0.98	0.24	0.49	–	–	–	–	–	–	–	–
Ciprofloxacin	–	–	–	–	15.63	3.9	1.95	–	–	–	–
Amphotericin B	–	–	–	–	–	–	–	0.98	3.9	0.49	0.49
Vancomycine	–	–	–	3.9	–	–	–	–	–	–	–

Results are mean values from at least three experiments; **(NA)** means no activity.

compounds, and the cell viability was assessed, using the MTT method. Data are presented as IC_{50} (μg/mL) values.

2.2.3. In vitro histone deacetylase (HDACs) inhibitory activity

The selective HDAC inhibitors provide a powerful chemical tool to dissect the individual functions of the HDAC isoforms and finally provide lead antitumor drug candidates. To assess the isoform selectivity of the 8-ethoxy-3-nitro-2H-chromene analogues, HDAC1 and HDAC2, representing class I, and HDAC8, representing class II, were used in the *in vitro* inhibitory assay. Only the analogs exhibiting potent cytotoxic effects were used in the assay: **7a**, **7c**, **7d**, **7i**, **7j**, **7 l**, and **7 m**, in comparison with the referenced HDAC inhibitor Vorinostat. The IC_{50} values for the selected compounds that displayed relatively good inhibitory activity toward HADC1, 2, and 8 at 10 μM had been determined in Table 4. As can be witnessed in Table 4, the chromene analogues **7d**, **7i**, and **7 l** manifested inhibitory activities against HDAC1 and 2 at, mostly, micromolar and submicromolar concentrations of 0.92–12.86 μM with a selective tendency towards HDAC1 and 2. For example, compounds **7d** had IC_{50} values of 1.94 and 2.53 for HDAC 1 and 2, respectively. In contrast, the chromene analogue **7 l** displayed effective inhibitory activity against HDAC1 over HDAC2 and HDAC8. In addition, the enzyme inhibitory activities of the most desired compounds were well-correlated with their antiproliferative activities. Compounds **7a**, **7c**, **7d**, **7i**, **7j**, **7 l**, and **7 m** with stronger antiproliferative activities also exerted higher inhibitory activities against the HDACs.

The perceptible rationale behind compound 7d exhibiting non-selectivity against HDAC1 and 2 is attributable to the electron-withdrawing substituents on the aryl moieties, acetyl and 4-fluro. In

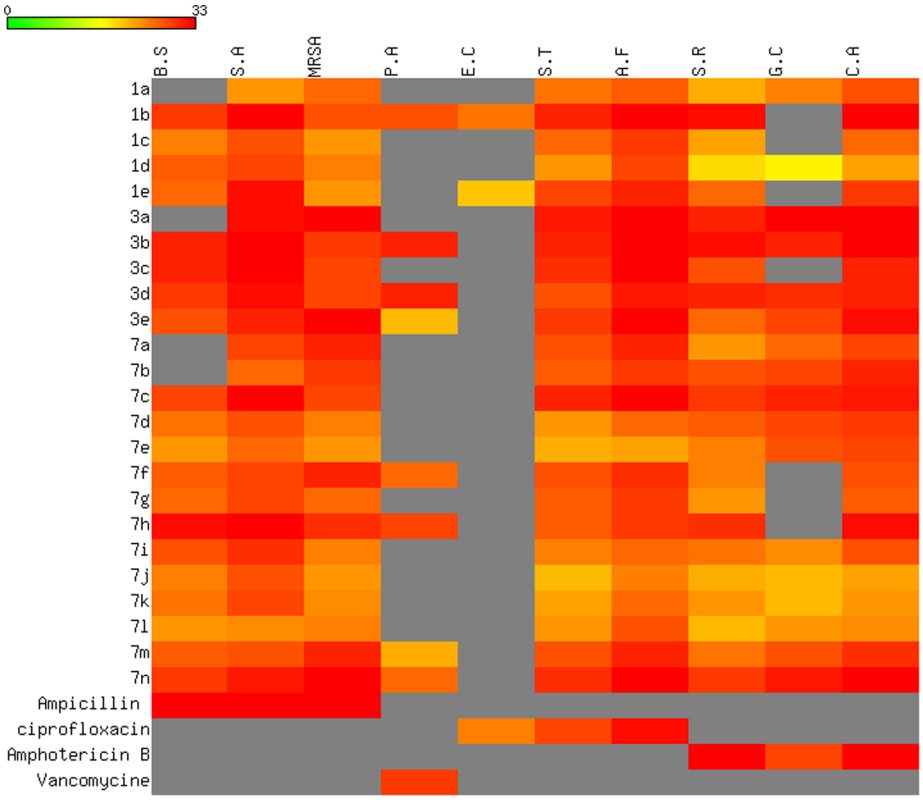

Fig. 2. Inhibition zone values (IZ) are reported for systematic compound comparisons. The values are color-coded, according to the following scheme: red 23–33, yellow 18–22, green < 15, and grey (not tested). The color bars mark the matrix positions of the compounds in a particular bacteria type: gm +ve, gm −ve, fungi, and MRSA.

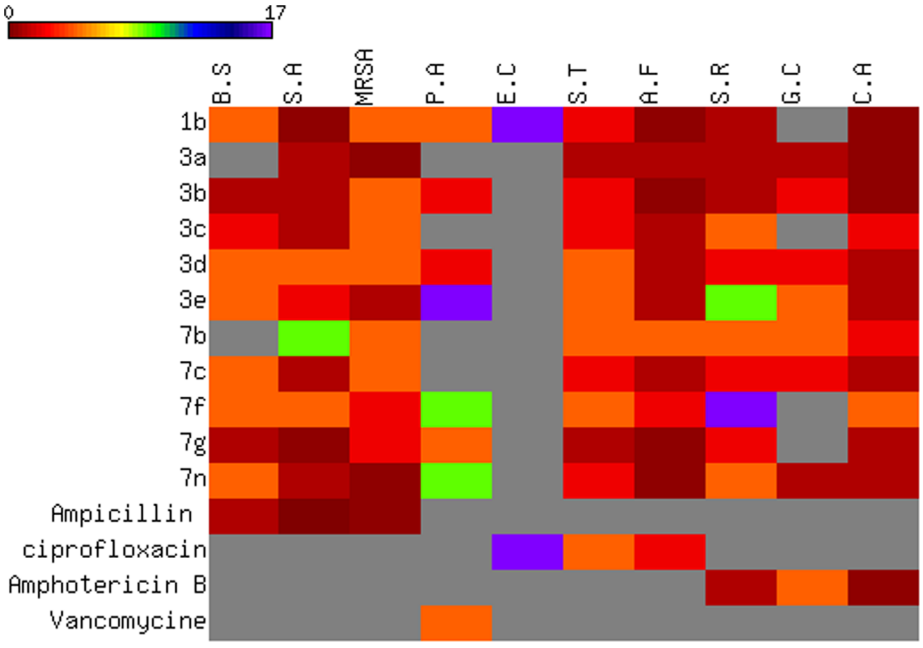

Fig. 3. Minimum inhibitory concentration values (MIC). The values are color-coded, according to the following scheme: spectrum colors; violet to yellow to green 6–10, blue to violet 14–17, and red > 5, with the grey color indicating missing data. The color bars mark the matrix positions of the compounds in a particular bacteria type: Gram positive, Gram negative, fungi, and MRSA.

contrast, the derivatives 7i and 7 m with a 4-CH_3 substituent as an electron-donating group, accompanied by the heteroaryl, thiazol, and oxazole moieties, presented selectivity tendencies towards HDAC1 only. Considering the obtained biological data, we could preliminarily arrive at the conclusion that some target compounds might be potent HDAC enzyme inhibitors. Thus, they assemble promising lead compounds for the development of novel anti-tumor drugs that can potentially alter the disease state via inhibiting HDACs.

2.2.4. Tubulin inhibitory effect screening

Microtubule-targeting agents affect microtubule functions and hinder the mitosis process, resulting in necrosis and apoptosis. Throughout our investigation, we delve into the influence of two chosen derivatives on the Tubulin polymerization, using the HCT-116 cancer cell line. The data exhibited a moderate effect on the inhibition of the Tubulin polymerization in comparison to Colchicine, reported in Table 5. As witnessed from the table, the derivative 7c with an electron-donating substituent (4-CH_3) demonstrated more activity in the selective comparison with 7d with an electron-withdrawing group (4-F) for the inhibition of the Tubulin polymerization. The intention of selecting 7c and 7d for this evaluation was as they are prime instances of selectivity and non-selectivity against the HDAC behavior, which is

Table 4
Cytotoxicity of the chromene derivatives against the three cancer cell lines.

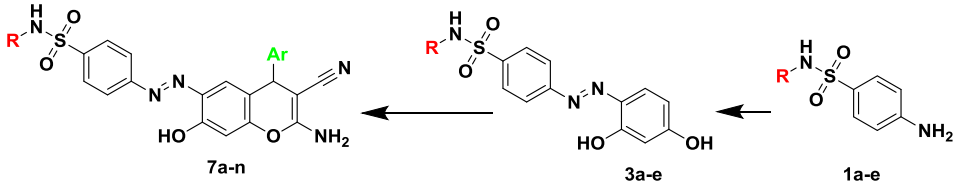

Compounds	R	Ar	IC_{50} (μM)		
			HCT-116	MCF-7	HepG-2
1a	**H**	**–**	93.5	143.43	256.1
1b	$COCH_3$	–	113.4	105.9	90.6
1c	NH_2–C═(NH)–	–	97.1	104.5	204.9
1d	Thiazol-2-yl	–	79.9	81.8	89.3
1e	3-methyl-isoxazol-5-yl		67.1	67.1	84.5
3a	H	–	39.5	40.2	60.7
3b	$COCH_3$	–	23.5	24.6	26.1
3c	NH_2–C═(NH)–	–	62.0	55.2	89.7
3d	Thiazol-2-yl	–	58.2	58.4	75.4
3e	3-methyl-isoxazol-5-yl	–	48.1	42.7	51.8
7a	H	C_6H_5	4.3	1.8	9.7
7b	H	C_6H_4F-4	11.8	9.6	10.1
7c	$COCH_3$	$C_6H_4CH_3$-4	8.3	5.6	9.8
7d	$COCH_3$	C_6H_4F-4	5.4	5.7	5.3
7e	$COCH_3$	C_6H_4Cl-2	11.8	17.9	15.1
7f	NH_2–C═(NH)–	C_6H_5	39.8	37.2	45.3
7g	NH_2–C═(NH)–	C_6H_4Cl-2	10.3	13.0	10.4
7h	NH_2–C═(NH)–	C_6H_4F-4	5.3	10.3	4.4
7i	Thiazol-2-yl	$C_6H_4CH_3$-4	10.6	9.5	11.3
7j	Thiazol-2-yl	C_6H_4F-4	5.5	4.7	5.5
7k	Thiazol-2-yl	C_6H_4Cl-2	14.8	18.9	13.4
7l	3-methyl-isoxazol-5-yl	$C_6H_4CH_3$-4	4.8	8.6	4.7
7m	3-methyl-isoxazol-5-yl	C_6H_4F-4	3.4	2.2	1.7
7n	3-methyl-isoxazol-5-yl	C_6H_4Cl-2	12.6	13.0	8.9
Doxorubicin	–		1.6	1.9	2.2

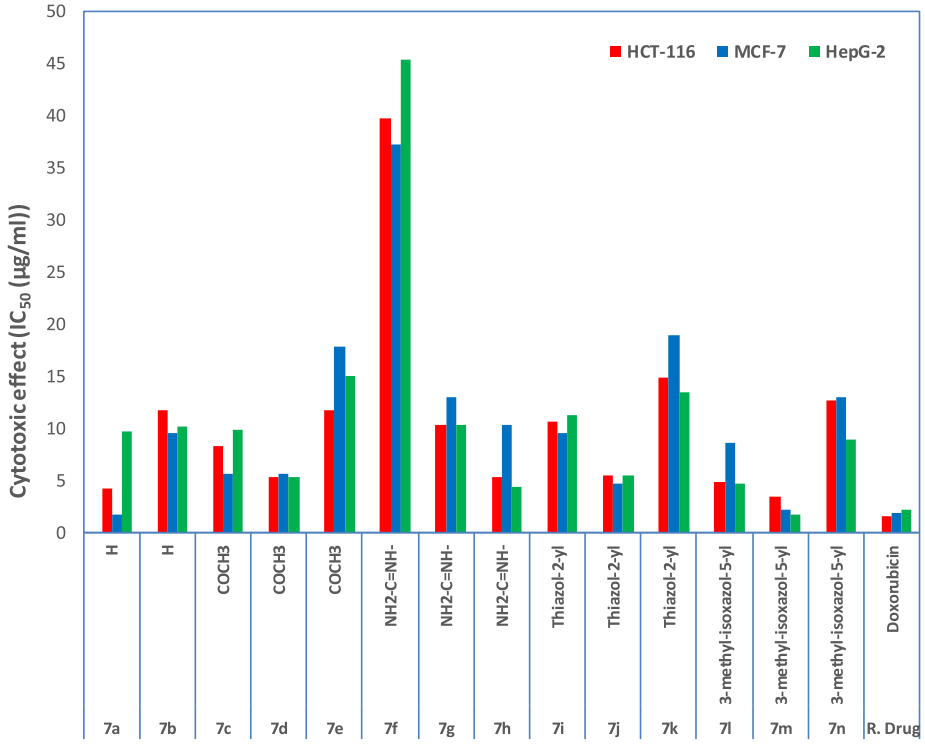

Fig. 4. *In vitro* cytotoxic activity. The IC_{50} values of the target compounds were introduced in the bar shape for the comparison of the effect of the aryl substitution on the chromene derivatives versus the reference drug.

Table 5
The inhibitory effect analyses of chromene derivatives against the HDAC classes and the Tubulin polymerization.

Compounds	Inhibitory activity				
	HDAC (IC_{50}, μM)			Tubulin polymerization	
	Class I Class II				
	HDAC1	HDAC2	HDAC8	HCT-116 (μM)	Inhibition %
7a	3.82	4.74	7.2	–	–
7c	7.18	**4.4**	> 10	7.18	92.44
7d	**1.94**	**2.53**	9.5	**8.84**	**87.12**
7i	**1.36**	3.64	> 10	–	–
7j	3.82	1.2	> 10	–	–
7l	**0.92**	12.86	> 100	–	–
7m	7.18	5.01	6.5	–	–
Vorinostat	0.82	0.93	1.98	–	–
Colchicine	–	–	–	0.16	86.3

Data are presented as average IC_{50} (μM) values for at least three experiments.

perceptible from the HDAC activity panel.

2.3. Docking studies of 7d, 7i, and 7 m into the HDAC2 enzyme

To further investigate the interactions between these compounds and the HDACs, we performed the docking simulations, using the MOE Suite. Following the ligand preparation, the compounds were docked into the binding pockets in the HDAC2 isoform as an example of class I HDACs. As shown in Fig. 5A (PDB ID: 4LY132) [46], the docking simulations suggested that the chromene compounds **7d**, **7i**, and **7 m** interact with the active site in a fashion similar to the benzamide ligand observed in the reported crystal structure of the HDAC 2 (PDB ID: 4LXZ), Fig. 5. Firstly, the docking pose of the benzamide ligand in the complex with HDAC2, Fig. 5A, consists of a long, narrow tunnel, leading to a cavity that contains the catalytic Zn^{2+} ion, which is pentacoordinated with Asp181, His183, and Asp269 as well as with the carbonyl oxygen and the NH_2 of the benzamide. In addition to the simultaneous bidentate chelate formation with Zn^{2+}, there is also a hydrogen bonding interaction with His145, Asp181, and Tyr308 through its benzamide NH and NH_2 fragments. According to the detailed interaction analyses reported in Table 6, the active derivatives **7d**, **7i** and **7 m** chelate mainly to the Zn^{2+} ion through its sulfonamide group by dual metal interactions. In addition, these molecules experienced interesting hydrogen bonding interactions with three important amino acid residues Tyr308, Gly154, and His146 through the NH and SO_2 fragments by a 1.5–3.1 Å distance range. Moreover, the aryl chromene moiety forms a π-π interaction with certain aromatic amino acids: Pro211, Phe155, Phe210, Leu276, and Tyr209, with the p-position substituents (F and Methyl) that might play an important role in increasing their binding affinity for the HDAC2 enzyme. This interaction analyses represented the role of the aryl substitution in HDAC selectivity and might be responsible for their antiproliferative effects.

The data reported in the table are extracted from MOE program showing the corresponding amino acids residues in enzyme pocket, corresponding fragments of ligands, interaction distances, types of interaction, and their binding energy to selected drugs.

3. Conclusion

This research depicts a breakthrough of a novel series of azosulfonamides bearing *4H*-chromenes, which were designed, synthesized, and evaluated for their inhibitory activity against the HCT-116, MCF-7, and HepG-2 cell lines. The incorporation of the chromene moieties into the azosulfonamide molecules instigated a substantial triumph in their cytotoxicity evaluation against their corresponding precursors. Furthermore, some of these 4*H*-chromene/sulfonamide derivatives displayed potent antiproliferative activities and were more potent towards the examined tumor cell lines in comparison to the Doxorubicin reference drug. Additionally, certain mechanisms were explored such as the HDAC inhibitory analyses, which established the existence of the submicromolar inhibitory concentrations against the HDAC 1 and 2 subtypes. In order to gain insight into the inhibition procedure of the HDAC enzymes and to verify the ligand-binding interactions, the blind docking protocol was adopted. The application of the sulfa drugs as both a zinc binding group (ZBG) and internal cavity motifs, attached to the chromene substructure, demonstrated high potential as potent anticancer molecules, mediated through the selective HDAC inhibition. To broaden our comprehensive study, we administrated assessments for the novel derivatives' antibacterial, antifungal, and antimycobacterium activities, which illustrated palpable bacterial and fungal inhibition when employing an evaluation against the reference drugs.

4. Experimental

4.1. Chemistry

The starting reagents and solvents were purchased from the Aldrich chemical company and were used as received. The melting points were determined with a Mel-Temp apparatus and are uncorrected. All the new compounds were characterized by the ^{1}H NMR and ^{13}C NMR, using Varian Gemini NMR spectrometer (Varian, Inc., Palo Alto, CA) (300 MHz, internal standard: tetramethylsilane), and ^{1}H NMR (400 MHz), ^{13}C NMR (100 MHz) and ^{13}C DEPT at 135° and ^{19}F NMR spectra on a Gemini 200 NMR spectrometer, and were measured in DMSO-d_6 at room temperature. The chemical shifts (δ) were reported in ppm to a scale calibrated for tetramethylsilane (TMS), which is used as an internal standard. The IR spectra (KBr pellets) were recorded using a FTIR Bruker Vector 22 spectrophotometer (Bruker Corp., Billerica, MA) (ν max in cm^{-1}) at the Microanalytical Center, Faculty of Science, Cairo University. The mass spectra were determined on a Shimadzu GC/MS-QP5050A spectrometer. Elemental analysis was carried out at the Regional Center for Mycology and Biotechnology (RCMP), Al-Azhar University, Cairo, Egypt and the results were within ± 0.25%. The follow up of the reactions and the check of the purity of the compounds were made by the TLC on silica gel-protected aluminum sheets (Type 60 GF254, Merck), and the spots were detected by exposure to a UV-lamp at λ 254 nm for a few seconds.

4.1.1. General procedure for the synthesis of 4-((2,4-dihydroxyphenyl) diazenyl)benzenesulfonamide (3a–e)

4-Aminobenzenesulfonamide(**1a–e**) (10 mmol) was suspended in water (50 mL). HCl (10 mL, 36.5%) was added dropwise to this solution with stirring. The mixture was gradually heated up to 70 °C till a clear solution was obtained. The solution was cooled to 0–5 °C in an ice bath. A sodium nitrite solution (0.5 g in 5 mL H_2O) was then added over a period of 5 min with stirring. Resorcinol (1.1 g, 10 mmol) was dissolved in 10% of the NaOH solution and kept at 0–5 °C. Subsequently, the diazonium salt solution was added with the occasional slow stirring to the resorcinol solution for 15–30 min. After acidification, the formed precipitate was filtered, dried, and recrystallized from absolute ethanol to give the pure products **3a–e**.

4-((2, 4-dihydroxyphenyl)diazenyl)benzenesulfonamide (3a)

Yellow crystals (87%), m.p. 130 °C; IR (KBr) cm^{-1}: υ_{max} 3518 (OH), 3401, 3180 (NH_2), 1627 (N═N), 1328, 1156 (S═O); ^{1}H NMR (DMSO-d_6, ppm) δ: 1.95 (2H, s, NH_2, D_2O exchangeable),6.38 (1H, s, Ar-H), 6.65 (2H, d, $J = 7$ *Hz*, Ar-H), 7.45 (1H, s, OH, D_2O, exchangeable) 7.68 (2H, d, $J = 7$ *Hz*, Ar-H), 7.97 (3H, m, Ar-H), 12.18 (1H, s, NH, D_2O exchangeable); ^{13}C NMR (DMSO-d_6, ppm) δ: 104.2, 107.5, 122.1, 124.4, 126.3, 131.2, 140.5, 153.1, 154.6, 160.1 (Ar-C). MS (*m/z*), 293; *Anal.* Calcd; for $C_{12}H_{11}N_3O_4S$: %C: 49.14, %H: 3.78; %N: 14.33. Found: %C: 49.10, %H: 3.64; %N: 14.41.

***N*-((-4-[(2,4-dihydroxyphenyl) diazenyl)phenyl) sulfonyl)**

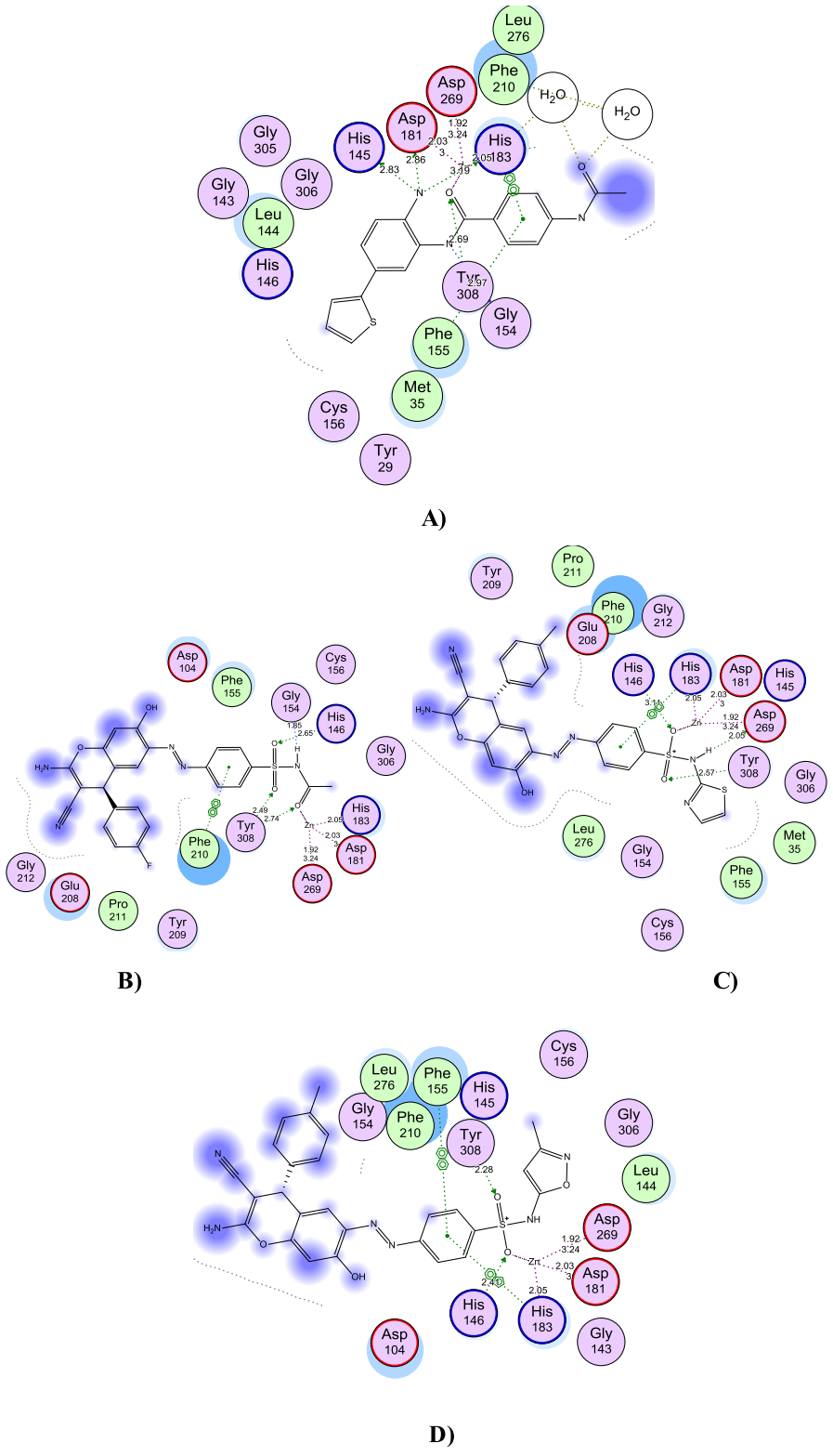

Fig. 5. Docking modes of active compounds in the binding pocket of HDAC2. Interactions between the protein (PDB ID: 4LY1), the ligands of compound **7d**, **7i**, **7m**, and the benzamide inhibitor are shown as dotted lines; the zinc ion as a black ion; the residues as colored codes as presented in the software; and the ligands as black line models. (A) Predicted binding mode of benzamide inhibitor with HDAC2. (B) Predicted binding mode of **7d** with HDAC2. (C) Predicted binding mode of **7i** with HDAC2. (D) Predicted binding mode of **7m** with HDAC2.

acetamide (3b)

Red crystals (84%), m.p. 150 °C; IR (KBr) cm^{-1}: υ_{max} 3480 (OH), 3250 (NH), 1625(C═O), 1597 (N═N), 1308, 1142 (S═O); ^{1}H NMR (DMSO-d_6, ppm) δ: 2.25 (3H, s, CH_3), 6.20 (1H, s, OH, D_2O exchangeable), 6.35 (1H, d, J = 7.1 *Hz*, Ar-H), 6.50 (1H, d, Ar-H), 6.72 (1H, s,Ar-H), 7.66 (1H, d, J = 7.1 *Hz*, Ar-H), 7.97 (2H, d, J = 8.4 *Hz*, Ar-H), 8.12 (2H, d, J = 8.4 *Hz*, Ar-H), 10.6 (1H, s, OH, D_2O exchangeable), 12.30 (1H, s, NH, D_2O exchangeable); ^{13}C NMR (DMSO-

Table 6
Description of the docking data of selected target compounds.

Comp.	Fragment	Target residues(distance, Å)	Interaction	Binding energy (dG)
7d	Acetyl C═O	**Zn + 2 (Asp269, Asp181, His183), 1.92, 2.03, 2.05**	Coordination bonding	−16.5
		Tyr308, 2.74		
	Sulphonamide- SO2	**Tyr308, 2.74**	Hydrogen bonding	
		His146, 2.65	Hydrogen bonding	
	Sulphonamide- NH	Gly154, 1.85	Hydrogen bonding	
	Sulphonamide- Benzene	Phe210, Phe155, , Tyr308	Hydrophobic interaction	
	Chromene	Asp104, Pro211, Glu208	Hydrophobic	
7i	Thiazole	Phe155, Met35	Hydrophobic	
	Sulphonamide- SO2	**Zn + 2 (Asp269, Asp181, His183), 1.92, 2.03, 2.05**	Coordination bonding	−16.4
		His146, 3.11	Hydrogen bonding	
		Tyr308, 2.57		
	Sulphonamide- NH	Asp269, 2.05	Hydrogen bonding	
	Sulphonamide- Benzene	His183, Leu276	Aromatic stacking	
	Chromene	Pro211, Phe210, Tyr209	Hydrophobic	
7l	Isoxazole	Leu144, Cys156, Gly306	Hydrophobic	−15.6
	Sulphonamide- SO2	**Zn + 2 (Asp269, Asp181, His183), 1.92, 2.03, 2.05**	Coordination bonding	
		His146 , 2.41	Hydrogen bonding	
		Tyr308, 2.28		
	Sulphonamide- Benzene	His183, Phe155, Phe210	Aromatic stacking	
	Chromene	Asp104, Gly154, Leu276	Hydrophobic	
Benzamide	Benzamide ring	His183, Tyr308, Phe155	Aromatic stacking	−14.5
	Benzamide C═O	**Zn + 2 (Asp269, Asp181), 3.19, 2.69**	Coordination bonding	
	Aniline NH2	**Tyr308, 2.69**	Hydrogen bonding	
		His145, 2.83	Hydrogen bonding	
		Asp181, 2.85	Hydrogen bonding	
		His185, 3.7	Hydrogen bonding	
	Thiophene	His146, Phe155, Leu144	Hydrophobic interaction	

d_6, ppm) δ: 16.2 (CH_3), 104.1, 107.3, 122.6, 124.5, 126.2, 130.2, 140.3, 156.5, 152.1, 160.5 (Ar-C), 170.10 (C═O). MS (*m/z*), 335; *Anal.* Calcd; for $C_{14}H_{13}N_3O_5S$: %C: 50.14, %H: 3.91; %N: 12.53. Found: %C: 65.23, %H: 3.82; %N: 12.63.

***N*-carbamimidoyl-4-((2,4-dihydroxyphenyl) diazenyl) benzenesulfonamide (3c)**

Orange crystals (92%), m.p. 136 °C; IR (KBr) cm^{-1}: υ_{max} 3594, 3436, 3338 (OH, NH, NH_2), 1626 (N═N), 1340, 1132 (S═O); ^{1}H NMR (DMSO-d_6, ppm) δ: 6.41 (1H, bs, Ar-H), 6.55 (1H, d, J = 7.1 *Hz*, Ar-H), 6.89 (2H, bs, NH_2), 7.69 (1H, d, J = 7.1 *Hz*, Ar-H), 7.93 (4H, bs, Ar-H), 9.80 (1H, s, OH, D_2O exchangeable), 10.6 (1H, s, NH, D_2O exchangeable), 12.80 (1H, s, NH, D_2O exchangeable); ^{13}C NMR (DMSO-d_6, ppm) δ: 103.0, 109.6, 121.7, 126.9, 129.6, 132.1, 144.1, 152.5, 157.2, 157.9 (Ar-C), 163.9 (C═N). ^{13}C NMR-DEPT (135°) δ: 102.8, 109.4, 121.5, 126.5, 126.7, 129.4 for ArCH's. MS (*m/z*), 335; *Anal.* Calcd; for $C_{13}H_{13}N_5O_4S$: %C: 46.56, %H: 3.91; %N: 20.88. Found: %C: 46.63, %H: 3.73; %N: 20.90.

4-((2,4-Dihydroxyphenyl) diazenyl)-*N*-(thiazol-2-yl) benzenesulfonamide (3d)

Orange crystals (89%), m.p. 133 °C; IR (KBr) cm^{-1}: υ_{max} 3447 (OH), 3150 (NH), 1623 (N═N), 1326, 1142 (S═O); ^{1}H NMR (DMSO-d_6, ppm) δ: 6.38 (1H, s, ArH), 6.52 (1H, d, J = 7.1 *Hz*, Ar-H), 6.84(1H, d, Ar-H), 7.25 (1H, d, J = 8 *Hz*, thiazol-H), 7.68 (1H, d, J = 8 *Hz*, thiazole-H), 7.94 (4H, bs, Ar-H), 9.46 (1H, s, OH, D_2O exchangeable), 12.27 (1H, bs, NH, D_2O exchangeable); ^{13}C NMR (DMSO-d_6, ppm) δ: 102.9, 108.2, 109.5, 121.7, 124.3, 126.9, 129.2, 132.6, 142.4, 152.4, 157.3, 163.9, 168.8 (Ar-C); ^{13}C NMR-DEPT (135°) δ: 102.6, 108.0, 109.3, 121.5, 124.1, 126.7, 128.9 for ArCH's. MS (*m/z*), 376; *Anal.* Calcd; for $C_{15}H_{12}N_4O_4S_2$: %C: 47.86, %H: 3.21; %N: 14.88. Found: %C: 47.70, % H: 3.34; %N: 14.78.

4-((2,4-Dihydroxyphenyl)diazenyl)-*N*-(3-methylisoxazol-5-yl) benzenesulfonamide (3e)

Red crystals (82%), m.p. 153 °C; IR (KBr) cm^{-1}: υ_{max} 3422 (OH), 3150 (NH), 1616 (N═N), 1346, 1154 (S═O); ^{1}H NMR (DMSO-d_6, ppm) δ: 2.30 (3H, s, CH_3), 6.17 (1H, s, ArH), 6.30 (1H, d, J = 7.1 *Hz*, Ar-H), 6.50(1H, d, Ar-H), 6.39 (1H, s, isoxazole-H), 7.67 (1H, d, J = 7.1 *Hz*, Ar-H), 8.01 (4H, bs, Ar-H), 10.70 (1H, s, OH, D_2O exchangeable), 11.50 (1H, s, NH, D_2O exchangeable); 12.1 (1H, bs, NH, D_2O exchangeable); ^{13}C NMR (DMSO-d_6, ppm) δ: 11.98(CH_3), 95.4, 103.0, 109.8, 122.1, 128.2, 128.9, 132.9, 139.3, 153.5, 157.3, 157.9, 164.4 (Ar-C). ^{13}C NMR-DEPT (135°) δ: 95.2, 102.7, 109.6, 121.9, 127.8, 128.6 for ArCH's. MS (*m/z*), 374; *Anal.* Calcd; for $C_{16}H_{14}N_4O_5S$: %C: 51.33, %H: 3.77; %N: 14.97. Found: %C: 51.30, %H: 3.82; %N: 14.86.

4.1.2. General procedure for the synthesis of 4-(2-amino-3-cyano-4-aryl-7-hydroxy-4-aryl-4H-chromen-6-yl)diazenyl] benzenesulfonamides (7a–n)

To a mixture of 4-((2, 4-dihydroxyphenyl)diazenyl)benzenesulfonamide (**3a–e**) (10 mmol) and arylidenemalononitriles (**5a–d**) (10 mmol) in 20 mL ethanol, a few drops of piperidine was added. The reaction mixture was refluxed for 1 h. After cooling, the precipitate was filtered, washed with water, and recrystallized from the appropriate solvent to yield the pure products **7a–n**.

4-((2-Amino-3-cyano-7-hydroxy-4-phenyl-4*H*-chromen-6-yl) diazenyl) benzenesulfonamide (7a)

Brown crystals (86%), m.p. 165 °C (EtOH); IR (KBr) cm^{-1}: υ_{max} 3439 (OH), 3357, 3203 (NH_2), 2190 (CN), 1589 (N═N), 1341, 1152 (S═O); ^{1}H NMR (DMSO-d_6, ppm) δ: 4.77 (1H, s, pyran-H), 6.80 (1H, d, Ar-H), 7.05 (2H, bs, NH_2, D_2O exchangeable), 7.18–7.20 (2H, m, Ar-H), 7.22–7.33 (2H, m, Ar-H),7.76 (1H, d, Ar-H), 8.02 (2H, d, Ar-H), 8.14 (2H, d, Ar-H), 11.97 (1H, s, NH, D_2O exchangeable); ^{13}C NMR (DMSO-d_6, ppm) δ: 28.5 (pyran-CH), 60.1, 104.1, 116.1 (CN), 123.1, 124.5, 125.2, 126.0, 128.1, 129.0, 129.3, 132.3, 140.1, 142.1, 148.2, 154.2, 160.1, 170.5 (Ar-C + pyran-*C*2 & pyran-C3). MS (*m/z*), 447; *Anal.* Calcd; for $C_{22}H_{17}N_5O_4S$: %C: 59.05, %H: 3.83; %N: 15.65. Found: %C: 59.15, %H: 3.63; %N: 14.53.

4-((2-Amino-3-cyano-7-hydroxy-4-(4-fluorophenyl)-4*H*-chromen-6- yl) diazenyl) benzene sulfonamide (7b)

Brown crystals (83%), m.p. 210 °C (EtOH); IR (KBr) cm^{-1}: υ_{max} 3495 (OH), 3355, 3180 (NH_2), 2193 (CN), 1604 (N═N), 1340, 1153 (S═O); ^{1}H NMR (DMSO-d_6, ppm) δ: 4.80 (1H, s, pyran-H), 6.81 (1H, d, Ar-H), 7.07–7.26 (4H, m, Ar-H and NH_2; D_2O exchangeable), 7.94 (2H, d, J = 7 Hz, Ar-H), 8.02 (2H, d, J = 7 Hz, Ar-H), 8.02 (2H, d, J = 7 Hz, Ar-H), 11.97 (1H, s, NH, D_2O exchangeable); ^{13}C NMR (DMSO-d_6, ppm) δ: 29.0 (pyran-CH), 59.1, 105.1, 115.1, 116.0, 117.1 (CN), 123.2, 124.1, 124.6, 130.2, 133.9, 137.1, 140.5, 148.1, 154.1, 159.2, 160.3, 177.1 (Ar-C + pyran-*C*2 & pyran-C3). MS (*m/z*), 465; *Anal.* Calcd; for

$C_{22}H_{16}FN_5O_4S$: %C: 56.77, %H: 3.46; %N: 15.05. Found: %C: 56.67, %H: 3.32; %N: 15.10.

***N*-4-((2-amino-3-cyano-7-hydroxy-4-(p-tolyl)-4*H*-chromen-6-yl) diazenyl)phenyl)sulfonyl) acetamide (7c)**

Orange crystals (83%), m.p. 155 °C (EtOH); IR (KBr) cm^{-1}: υ_{max} 3490 (OH), 3350, 3150 (NH_2), 2217 (CN), 1723 (C═O), 1598 (N═N), 1367, 1143 (S═O); ^{1}H NMR (DMSO-d_6, ppm) δ: 2.18 (3H, s, $COCH_3$), 2.38 (3H, s, Ar-CH_3), 5.06 (1H, s, pyran-H), 6.84 (1H, s, Ar-H), 6.99 (1H, d, Ar-H), 7.05 (2H, d, Ar-H), 7.19(1H, S, NH), 7.39 (2H, d, Ar-H), 7.93(2H, d, Ar-H), 8.33(1H, s, Ar-H), 8.05(1H, s, NH, D_2O exchangeable), 12.13 (1H, s, NH (Hydrazo), D_2O exchangeable); ^{13}C NMR (DMSO-d_6, ppm) δ: 16.1 (CH_3), 21.1 (CH_3), 30.1 (pyran-CH), 59.5, 105.1, 116.0 (CN), 121.9, 124.2, 124.5, 125.3, 128.1, 129.6, 134.1, 134.3, 138.5, 140.3, 150.1, 154.1, 160.1, 172.5 (Ar-C + pyran-*C*2 & pyran-C3), 176.4 (C═O). MS (*m/z*), 503; *Anal.* Calcd; for $C_{25}H_{21}N_5O_5S$: %C: 59.63, %H: 4.20; %N: 13.91. Found: %C: 59.52, %H: 4.37; %N: 13.97.

***N*-4-((2-amino-3-cyano-4-(4-fluorophenyl)-7-hydroxy-4*H*-chromen-6-yl)diazenyl) phenylsulfonyl) acetamide (7d)**

Orange crystals (85%), m.p. 162 °C (EtOH); IR (KBr) cm^{-1}: υ_{max} 3412 (OH), 3316, 3188 (NH_2), 2192 (CN), 1700 (C═O), 1604 (N═N), 1314, 1138 (S═O); ^{1}H NMR (DMSO-d_6, ppm) δ: 2.16 (3H, s, CH_3CO), 4.77 (1H, s, pyran-H), 6.39 (1H, s, Ar-H), 6.72 (1H, s, Ar-H), 6.73 (2H, d, Ar-H), 7.08–7.22(4H, m, Ar-H and NH_2), 7.74(2H, d, Ar-H), 7.96 (2H, d, Ar-H), 8.00 (2H, d, Ar-H), ^{13}C NMR (DMSO-d_6, ppm) δ: 21.1 (CH_3), 30.0 (pyran-CH), 58.8, 105.1, 115.1, 116.0 (CN), 123.1, 124.1, 124.6, 125.2, 128.1, 130.2, 134.2, 138.4, 140.1, 150.3, 155.3, 160.2, 173.0 (Ar-C + pyran-*C*2 & pyran-C3), 177.2 (C═O). MS (*m/z*), 507; *Anal.* Calcd; for $C_{24}H_{18}FN_5O_5S$: %C: 56.80, %H: 3.58; %N: 13.80. Found: %C: 56.91, %H: 3.45; %N: 13.70.

***N*-(4-((2-amino-4-(2-chlorophenyl)-3-cyano-7-hydroxy–4*H*-chromen-6-yl)diazenyl) phenylsulphonyl)acetamide (7e)**

Orange crystals (80%), m.p. 177 °C (EtOH); IR (KBr) cm^{-1}: υ_{max} 3447 (OH), 3350, 3100 (NH_2), 2193 (CN), 1690 (C═O), 1598 (N═N), 1398, 1150 (S═O); ^{1}H NMR (DMSO-d_6, ppm) δ: 2.23 (3H, s, CH_3CO), 5.29 (1H, s, pyran-H), 6.72 (1H, s, Ar-H), 6.79(1H, d, Ar-H), 7.05 (1H, s, NH, D_2O exchangeable), 7.09–7.41(4H, m, Ar-H and NH_2), 7.75 (1H, d, Ar-H), 8.08 (4H, br s, Ar-H), 11.86 (1H, s, NH, D_2O exchangeable); ^{13}C NMR (DMSO-d_6, ppm) δ: 20.4 (CH_3), 30.0 (pyran-CH), 58.8, 105.0, 117.0 (CN), 123.1, 124.1, 124.6, 125.6, 127.1, 127.3, 129.2, 129.7, 133.7, 141.2, 142.0, 148.0, 154.6, 173.0 (Ar-C + pyran-*C*2 & pyran-C3), 176.0 (C═O). Anal. Calcd; for $C_{24}H_{18}ClN_5O_5S$: %C: 55.02, %H: 3.46; %N: 13.37. Found: %C: 55.23, %H: 3.56; %N: 13.26.

4-((2-Amino-3-cyano-7-hydroxy-4-phenyl-4*H*-chromen-6-yl) diazenyl)-*N*-carbamimidoyl benzenesulfonamide (7f)

Orange crystals (88%), m.p. 156 °C (EtOH); IR (KBr) cm^{-1}: υ_{max} 3428 (OH), 3343, 3208 (NH_2), 2190 (CN), 1589 (N═N), 1398, 1137 (S═O); ^{1}H NMR (DMSO-d_6, ppm) δ: 4.78 (1H, s, pyran-H), 6.77 (2H, br, NH_2), 6.80 (1H, s, NH), 6.82 (1H, s, NH), 7.03 (2H, s, NH_2), 7.22 (3H, t, Ar-H), 7.31 (3H, t, Ar-H), 7.77 (1H, d, Ar-H), 7.9 (2H, d, Ar-H), 8.05 (2H, d, Ar-H), 11.90 (1H, s, NH); ^{13}C NMR (DMSO-d_6, ppm) δ: 36.3 (pyran-CH), 57.3, 108.4, 112.4 (CN), 119.9, 122.5, 124.2, 126.5, 126.6, 127.0, 128.3, 134.0, 144.0, 145.8, 151.9, 152.7, 153.4, 158.0, 159.4 (Ar-C + pyran-*C*2 & pyran-C3). ^{13}C NMR-DEPT (135°) δ: 36.0, 108.1, 122.2, 123.9, 126.2, 126.3, 126.7, 128.0 for ArCH′s. MS (*m/z*), 489; *Anal.* Calcd; for $C_{23}H_{19}N_7O_4S$: %C: 56.43, %H: 3.91; %N: 20.03. Found: %C: 56.55, %H: 3.84; %N: 20.12.

4-((2-amino-4-(2-chlorophenyl)-3-cyano-7-hydroxy-4*H*-chromen-6-yl)diazenyl)-*N*-carbamimidoylbenzenesulfonamide (7 g)

Orange crystals (86%), m.p. 182 °C (EtOH/Dioxane); IR (KBr) cm^{-1}: υ_{max} 3422 (OH), 3343, 3216 (NH_2), 2194 (CN), 1586 (N═N), 1398, 1139 (S═O); ^{1}H NMR (DMSO-d_6, ppm) δ: 5.30 (1H, s, pyran-H), 6.78 (2H, br, NH_2), 6.80 (2H, s, NH_2), 7.03 (2H, s, NH_2), 7.13 (1H, s, NH), 7.20–7.28(2H, m, Ar-H), 7.41 (1H, d, Ar-H), 7.77 (1H, d, Ar-H), 7.88(2H, d, Ar-H), 8.05(2H, d, Ar-H), 11.82(1H, s, NH Hydrazo); ^{13}C NMR (DMSO-d_6, ppm) δ: 33.4 (pyran-CH), 55.9, 108.0, 111.3 (CN), 119.4, 122.5, 123.6, 126.5, 127.5, 128.1, 129.2, 130.0, 131.9, 134.9, 141.2, 145.7, 152.1, 153.0, 153.09, 158.0, 159.4 (Ar-C + pyran-*C*2 & pyran-C3). ^{13}C NMR-DEPT (135°) δ: 33.4, 107.9, 122.3, 123.3, 126.3, 127.2, 127.8, 129.0, 129.8 for ArCH′s. Anal. Calcd; for $C_{23}H_{18}ClN_7O_4S$: %C: 52.72, %H: 3.46; %N: 18.71. Found: %C: 52.74, %H: 3.50; %N: 18.63.

4-((2-amino-3-cyano-4-(4-fluorophenyl)-7-hydroxy-4*H*-chromen-6-yl)diazenyl)-*N*-carbamimidoylbenzenesulfonamide (7 h)

Orange crystals (83%), m.p. 230 °C (EtOH); IR (KBr) cm^{-1}: υ_{max} 3427 (OH), 3342, 3209 (NH_2), 2191 (CN), 1588 (N═N), 1399, 1139 (S═O); ^{1}H NMR (DMSO-d_6, ppm) δ: 4.81 (1H, s, pyran-H), 6.76 (2H, b s, NH_2), 6.79 (1H, s, Ar-H), 6.82 (1H, s, NH), 7.05 (2H, s, NH_2), 7.13 (2H, t, Ar-H), 7.25 (2H, m, Ar-H), 7.77(1H, d, Ar-H), 7.89 (2H, d, Ar-H), 8.05(2H, d, Ar-H), 11.98 (1H, NH, Hydrazo); ^{13}C NMR (DMSO-d_6, ppm) δ: 35.7 (pyran-CH), 57.0, 108.4, 112.2, 114.9 (CN), 115.1, 119.8, 122.5, 124.0, 126.6, 128.8, 128.9, 134.9, 141.0, 145.8, 151.9, 152.5, 153.5, 158.0, 159.3, 159.5, 162.0 (Ar-C + pyran-*C*2 & pyran-C3). ^{13}C NMR-DEPT (135°) δ: 35.4, 108.1, 114.6, 114.8, 122.2, 123.8, 126.3, 128.6, 128.7 for ArCH′s. MS (*m/z*), 507; *Anal.* Calcd; for $C_{23}H_{18}FN_7O_4S$: %C: 54.43, %H: 3.57; %N: 19.32. Found: %C: 54.47, %H: 3.65; %N: 19.41.

4-((2-amino-3-cyano-7-hydroxy-4-p-tolyl-4*H*-chromen-6-yl)diazenyl)-*N*-(thiazol-2-yl) benzenesulfonamide (7i)

Orange crystals (82%), m.p. 175 °C (EtOH); IR (KBr) cm^{-1}: υ_{max} 3460 (OH), 3347, 3100 (NH_2), 2192 (CN), 1586 (N═N), 1328, 1142 (S═O); ^{1}H NMR (DMSO-d_6, ppm) δ: 2.23 (3H, s, Ar-CH_3), 4.72 (1H, s, pyran-H), 6.80 (1H, d, $J = 8\,Hz$, thiazole-H), 6.84 (1H, d, $J = 8\,Hz$, thiazole-H), 7.0 (2H, s, NH_2), 7.08 (4H, bs, Ar-H), 7.25(1H, dd, Ar-H), 7.55 (1H, dd, NH, Ar-H), 7.85 (1H, dd, NH, Ar-H), 7.93 (2H, d, Ar-H) 8.06 (2H, d, Ar-H), 8.44 (1H, S, OH), 12.07 (1H, bs, NH Hydrazo); ^{13}C NMR (DMSO-d_6, ppm) δ: 20.5 (CH_3), 36.1 (pyran-CH), 59.0, 80.0, 108.4, 108.6, 112.7 (CN), 120.0, 122.7, 126.9, 127.0, 128.9, 130.0, 135.0, 135.7, 141.9, 143.6, 145.6, 152.4, 152.8, 153.6, 159.4, 161.1, 168.8 (Ar-C + pyran-*C*2 & pyran-C3). ^{13}C NMR-DEPT (135°) δ: 35.8, 108.1, 108.3, 122.5, 124.1, 124.2, 126.6, 126.7, 128.6, 129.8, 130.3, 161.1 for ArCH′s. MS (*m/z*), 544; *Anal.* Calcd; for $C_{26}H_{20}N_6O_4S_2$: %C: 57.34, %H: 3.70; %N: 15.43. Found: %C: 57.27, %H: 3.73; %N: 15.52.

4-((2-amino-3-cyano-4-(4-fluorophenyl)-7-hydroxy-4*H*-chromen-6-yl)diazenyl)-*N*-(thiazol-2-yl) benzenesulfonamide (7j)

Orange crystals (93%), m.p. 166 °C (EtOH); IR (KBr) cm^{-1}: υ_{max} 3490 (OH), 3337, 3150 (NH_2), 2192 (CN), 1603 (N═N), 1328, 1142 (S═O); ^{1}H NMR (DMSO-d_6, ppm) δ: 4.80 (1H, s, pyran-H), 6.80 (1H, d, $J = 8\,Hz$, thiazole-H), 6.84 (1H, d, $J = 8\,Hz$, thiazole-H), 7.07 (2H, t, Ar-H), 7.22–7.27 (3H, m, Ar-H), 7.76 (1H, d, Ar-H), 7.93 (2H, d, Ar-H), 8.07 (2H, d, Ar-H),12.04 (1H, s, NH, hydrazo), 12.79 (1H, bs, NH); ^{13}C NMR (DMSO-d_6, ppm) δ: 35.8 (pyran-CH), 57.11, 108.45, 108.65, 112.38, 115.01, 115.22, 119.94 (CN), 122.83, 124.13, 124.50, 126.93, 128.97, 129.05, 135.07, 141.1, 143.61, 152.53, 152.78, 153.76, 159.43, 162.11, 168.94 (Ar-C + pyran-*C*2 & pyran-C3). ^{13}C NMR-DEPT (135°) δ: 35.57, 108.2, 108.39, 112.57, 114.76, 122.59, 123.85, 124.25, 126.68, 128.72, 128.8 for ArCH′s. MS (*m/z*), 548; *Anal.* Calcd; for $C_{25}H_{17}FN_6O_4S_2$: %C: 54.74, %H: 3.12; %N: 15.32. Found: %C: 54.73, %H: 3.20; %N: 15.37.

4-((2-amino-4-(2-chlorophenyl)-3-cyano-7-hydroxy-4*H*-chromen-6-yl)diazenyl)-*N*-(thiazol-2-yl) benzenesulfonamide (7 k)

Orange crystals (91%), m.p. 182 °C (EtOH); IR (KBr) cm^{-1}: υ_{max} 3424 (OH), 3331, 3100 (NH_2), 2188 (CN), 1589 (N═N), 1328, 1147 (S═O); ^{1}H NMR (DMSO-d_6, ppm) δ: 5.30 (1H, s, pyran-H), 6.79 (1H, d, $J = 8\,Hz$, thiazole-H), 6.82 (1H, d, $J = 8\,Hz$, thiazole-H), 7.03 (2H, s, NH_2), 7.12 (1H, d, Ar-H), 7.22–7.26 (3H, m, Ar-H), 7.41 (1H, d, Ar-H), 7.76 (1H, d, Ar-H), 7.91 (2H, d, Ar-H), 8.07 (2H, d, Ar-H), 11.89 (1H, s, NH); ^{13}C NMR (DMSO-d_6, ppm) δ: 33.7 (pyran-CH), 55.80, 108.3, 111.3, 119.4 (CN), 122.8, 123.4, 125.1, 126.8, 127.5, 128.2, 129.3, 130.14, 135.0, 141.9, 143.7, 152.5, 153.1, 154.0, 159.4, 168.0(Ar-

C + pyran-*C*2 & pyran-C3. ^{13}C NMR-DEPT (135°) *δ*: 33.50, 108.12, 122.6, 123.1, 124.8, 126.5, 127.3, 127.9, 129.1, 129.8 for ArCH's. Anal. Calcd; for $C_{25}H_{17}ClN_6O_4S$: %C: 53.14, %H: 3.03; %N: 14.87. Found: %C: 53.27, %H: 3.12; %N: 14.89.

4-((2-Amino-3-cyano-7-hydroxy-4-(p-tolyl)-4*H*-chromen-6-yl) azo] -*N*-(3-methyl isoxazol-2-yl) benzene sulfonamide (7 l)

Orange crystals (95%), m.p. 162 °C (EtOH); IR (KBr) cm^{-1}: υ_{max} 3420 (OH), 3366, 3150 (NH_2), 2193 (CN), 1614 (N═N), 1333, 1156 (S═O); ^{1}H NMR (DMSO-d_6, ppm) *δ*: 2.28 (3H, s, CH_3), 5.29 (1H, s, pyran-H), 6.15 (1H, s, isoxazole-H), 7.09 (2H, s, NH_2), 7.13–7.72 (11*H*, m, Ar-H + NH), 11.79 (1H, s, OH); ^{13}C NMR (DMSO-d_6, ppm) *δ*: 14.1 (CH_3), 33.5 (pyran-CH), 60.0, 105.0, 118.0 (CN), 122.0, 124.0, 124.1, 124.5, 126.1, 126.4, 127.0, 128.5, 129.2, 129.7, 134.0,140.0, 142.0, 148.0, 150.0, 155.0, 157.0, 160.0, 176.0 (Ar-C + pyran-*C*2 & pyran-C3). MS (*m/z*), 542; *Anal.* Calcd; for $C_{27}H_{22}N_6O_5S$: %C: 59.77, %H: 4.09; %N: 15.49. Found: %C: 59.82, %H: 4.01; %N: 15.55.

4-((2-amino-3-cyano-4-(4-fluorophenyl)-7-hydroxy-4*H*-chromen-6-yl)diazenyl)-*N*-(3-methyl isoxazol-2-yl) benzene sulfonamide (7 m)

Brown crystals (96%), m.p. 177 °C (EtOH); IR (KBr) cm^{-1}: υ_{max} 3446 (OH), 3350, 3154 (NH_2), 3010 (CH aromatic), 2840 (CH aliphatic), 2193 (CN), 1655 (N═N), 1333, 1157 (S═O) 1167 (C-F); ^{1}H NMR (DMSO-d_6, ppm) *δ*: 2.07 (2H, s, NH_2, D_2O exchangeable), 2.29 (3H, s, CH_3), 4.80 (1H, s, pyran-H), 6.17 (1H, s, isoxazole-H), 6.80(1H, d, Ar-H), 7.07 (2H, bs, NH_2), 7.12 (2H, d, Ar-H), 7.24, (2H, d, Ar-H), 7.75 (1H, d, Ar-H), 7.99 (2H, d, Ar-H), 11.52 (1H, s, NH), 11.94 (1H, s, NH, Hydrazo); ^{13}C NMR (DMSO-d_6, ppm) *δ*: 11.89 (CH_3), 35.84 (pyran-CH), 56.9, 108.7, 112.4, 115.0, 115.23 (CN), 119.9, 123.1, 123.4, 128.0, 128.9, 129.07, 135.2, 140.3, 141.1, 153.0, 153.3, 154.3, 157.3, 159.4, 170.4 (Ar-C + pyran-*C*2 & pyran-C3). ^{13}C NMR-DEPT (135°) *δ*: 35.58, 95.16, 108.5, 114.76, 114.97, 122.87, 123.16, 127.7, 128.73, 128.81 for ArCH's. ^{19}F NMR *δ*: −116.16. MS (*m/z*), 546; *Anal.* Calcd; for $C_{26}H_{19}FN_6O_5S$: %C: 57.14, %H: 3.50; %N: 15.38. Found: %C: 57.20, %H: 3.61; %N: 15.45.

4-((2-amino-4-(2-chlorophenyl)-3-cyano-7-hydroxy-4*H*-chromen-6-yl)diazenyl)-*N*-(3-methyl isoxazol-2-yl) benzenesulfonamide (7n)

Brown crystals (96%), m.p. 182 °C (EtOH); IR (KBr) cm^{-1}: υ_{max} 3420 (OH), 3366, 3150 (NH_2), 3060 (CH aromatic), 2193 (CN), 1655 (N═N), 1333, 1156 (S═O), 1083 (C-Cl); ^{1}H NMR (DMSO-d_6, ppm) *δ*: 2.29 (3H, s, CH_3), 5.30 (1H, s, pyran-H), 6.16 (1H, s, isoxazole-H), 6.79 (1H, s, Ar-H), 7.04, (2H, bs, Ar-H), 7.13 (1H, d, Ar-H), 7.21–7.26 (2H, m, Ar-H), 7.41 (1H, d, Ar-H), 7.74 (1H, d, Ar-H), 7.97 (2H, d, Ar-H), 11.49 (1H, s, OH), 11.93 (1H, s, NH); ^{13}C NMR (DMSO-d_6, ppm) *δ*: 11.95 (CH_3), 33.80 (pyran-CH), 55.8, 95.4, 108.5, 111.4, 119.4 (CN), 122.90, 123.1, 127.5, 128.2, 129.3, 132.0, 135.2, 140.3, 142.01, 153.4, 154.51, 157.3, 159.4, 170.05 (Ar-C + pyran-*C*2 & pyran-C3). ^{13}C NMR-DEPT (135°) *δ*: 33.54, 95.2, 108.26, 122.62, 122.91, 127.34, 127.67, 127.97, 129.11, 129.91 for ArCH's. Anal. Calcd; for $C_{26}H_{19}ClN_6O_5S$: %C: 55.47, %H: 3.40; %N: 14.93. Found: %C: 55.51, %H: 3.57; %N: 14.75.

4.2. Biological studies

4.2.1. Antimicrobial screening

The microorganism inoculums were uniformly spread, using sterile cotton swabs on a sterile Petri dish with malt extract agar (for fungi) and nutrient agar (for bacteria). One hundred cubic millimeters of each sample was added to each well (10-mm-diameter holes were cut in the agar gel, 20 mm apart from one another). The systems were incubated for 24–48 hr. at 37 °C (for bacteria) and at 28 °C (for fungi). After incubation, the microorganism's growth was observed. The inhibition zones of the bacterial and fungal growth were measured in millimeters. The tests were performed in a triplicate [35,36].

4.2.2. Cytotoxic screening

Human colon carcinoma (HCT-116), human hepatocellular carcinoma (HEPG-2),and human breast adenocarcinoma (MCF-7) cell lines were obtained from the American Type Culture Collection (ATCC, Rockville, MD). The cells were grown on RPMI-1640 medium supplemented with 10% inactivated fetal calf serum and 50 µg/mL gentamycin. The cells were maintained at 37 °C in a humidified atmosphere with 5% CO_2 and were subcultured two to three times a week. Potential cytotoxicity of the compounds was evaluated on tumor cells using the method of Gangadevi and Muthumary [37]. The cells were grown as monolayers in growth RPMI-1640. The monolayers of 104 cells adhered at the bottom of the wells in a 96-well microliter plate incubated for 24 h at 37 °C in a humidified incubator with 5% CO_2. The monolayers were then washed with sterile phosphate buffered saline (0.01 M pH 7.2) and simultaneously the cells were treated with 100 µL from different dilutions of tested sample in fresh maintenance medium and incubated at 37 °C. A control of untreated cells was made in the absence of tested sample. Positive controls containing doxorubicin were also tested as a reference drug for comparison. Six wells were used for each concentration of the test sample. Every 24 h′ observation under the inverted microscope was made. The number of the surviving cells was determined by staining the cells with crystal violet [38,39] followed by cell lysing using 33% glacial acetic acid and the absorbance read at 590 nm using a microplate reader (SunRise, TECAN, Inc, USA) through mixing. The absorbance values from untreated cells were considered as 100% proliferation. The number of viable cells was determined using microplate reader as previously mentioned and the percentage of viability was calculated as [1-(ODt/ODc)]x100% where ODt is the mean optical density of wells treated with the tested sample and ODc is the mean optical density of untreated cells. The relation between surviving cells and drug concentration wasplotted to get the survival curve of each tumor cell line after treatment with thespecified compound. The 50% inhibitory concentration (IC_{50}), the concentration required to cause toxic effects in 50% of intact cells, was estimated from graphic plots.

4.2.3. *In vitro* cell-based HDACs screening

The *In vitro* HDACs inhibition assays were conducted as previously described [40]. In brief, 10 µL of the enzyme solution (HDAC1, HDAC2, and HDAC8) was mixed with different concentrations of the selected 8-ethoxy-3-nitro-2H-chromene derivatives (50 µL), positive drug control SAHA and MS275, using 100% and none of the HDACs groups as control groups, and the mixture. After incubation at 37 °C for 10 min, the fluorogenic substrate Ac-Leu-GlyLys(Ac)-AMC (40 µL) was added and then the mixture was incubated at 37 °C for 30 min. The reaction was quenched with 100 µL of the stop buffer, containing trypsin and TSA. After incubation at 37 °C for 20 min, the fluorescence intensity was measured, using a microplate reader at the excitation and emission wavelengths of 390 and 460 nm, respectively. The inhibition ratios were calculated from the fluorescence intensity readings of the tested wells relative to those of the control wells. In the IC50 determination, each compound was tested at 8 concentrations, starting from 10 µ M with a 3-fold-dilution in a singlet. The IC50 values were calculated, using a regression analysis of the concentration/inhibition data [40].

4.2.4. Tubulin polymerization assay

The HCT-116 cell line was obtained from the American Type Culture Collection; they were cultured, using DMEM (Invitrogen/Life Technologies) and supplemented with 10% of FBS (Hyclone), 10 µ g/mL of insulin (Sigma), and 1% of penicillin–streptomycin. The plate cells (cells density 1.2–1.8 × 10,000 cells/well) in a volume of 100µ l complete growth medium and 100µ l of the tested compound per well in a 96-well plate for 18–24 h before the enzyme assay for Tubulin. The microtiter plate provided in this kit has been pre-coated with an antibody specific to TUBb. The standards or samples were then added to the appropriate microtiter plate wells with a biotin-conjugated antibody

specific to TUBb. Next, the Avidin conjugated to Horseradish Peroxidase (HRP) was added to each microplate well and incubated. After the TMB substrate solution was added, only those wells that contained TUBb, a biotin-conjugated antibody and enzyme-conjugated Avidin, exhibited a change in color. The enzyme-substrate reaction is terminated by the addition of the sulphuric acid solution, and the color change is measured spectrophotometrically at a wavelength of 450 nm ± 10 nm. The concentration of TUBb in the samples is then determined by comparing the O.D. of the samples to the standard curve. [41–43]

4.3. Molecular modeling

The newly synthesized compounds were docked into the HDAC 2 isoform as an example of the class II HDACs crystal structure of (PDB ID: 4LXZ). The AutoDock 3.0 [44] and the MOE software [45] were used for all the docking calculations. The AutoDock Tools [44] package was employed to generate the docking input files and to analyze the docking results. A grid box size of 90 × 90 × 90 points with a spacing of 0.375 Å between the grid points was generated that covered almost the entire protein surface. The ligands were fully flexibly docked. All the non-polar hydrogens and the crystal water molecules were removed prior to the calculations. The docking grid was centered on the mass center of the bound benzamide drug. In each case, 100 docked structures were generated, using the genetic algorithm searches. A default protocol was applied with an initial population of 50 randomly placed conformations, a maximum number of 2.5 × 105 energy evaluations, and a maximum number of 2.7 × 104 generations. A mutation rate of 0.02 and a crossover rate of 0.8 were used. The heavy atom comparison root mean square deviations (RMSD values) were calculated, and the initial ligand binding modes were plotted. The protein–ligand interaction plots were generated, using MOE 2012.10. The quantum mechanical calculations and the surface molecular orbitals were generated by the simulation module in the MOE software.

Acknowledgements

The authors wish to express outmost gratitude towards Malak T. Mahmoud for editing and revising the manuscript.

References

[1] A.K. Jindal, K. Pandya, I.D. Khan, Antimicrobial resistance: a public health challenge, Med. J. Armed Forces India 71 (2) (2015) 178–181.
[2] A. Beceiro, M. Tomas, G. Bou, Antimicrobial resistance and virulence: a successful or deleterious association in the bacterial world? Clin. Microbiol. Rev. 26 (2) (2013) 185–230.
[3] G.D. Goss, E. Tsvetkova, Drug resistance and its significance for treatment decisions in non-small-cell lung cancer, Curr. Oncol. 19 (2012) S45–S51.
[4] H. Maeda, M. Khatami, Analyses of repeated failures in cancer therapy for solid tumors: poor tumor-selective drug delivery, low therapeutic efficacy and unsustainable costs, Clin. Transl. Med. 7 (1) (2018) 1–20.
[5] H. Zahreddine, K.L.B. Borden, Mechanisms and insights into drug resistance in cancer, Front. Pharmacol. 4 (2013) 1–8.
[6] J. Mori, M. Iwashima, M. Takeuchi, H. Saito, A synthetic study on antiviral and antioxidative chromene derivative, Chem. Pharm. Bull. 54 (2006) 391–396.
[7] Y. He, Y.Y. Chen, J.B. Shi, W.J. Tang, Z.X. Pan, Z.Q. Dong, B.A. Song, J. Li, X.H. Liu, New coumarin derivatives: Design, synthesis and use as inhibitors of hMAO, Bioorg. Med. Chem. 22 (2014) 3732–3738.
[8] J. Charles, S.V. Michael, S.W. Gabriel, H.H. Amir, Zr-catalyzed kinetic resolution of allylic ethers and mo-catalyzed chromene formation in synthesis. enantioselective total synthesis of the antihypertensive agent (*S*,*R*,*R*,*R*)-nebivolol, J. Am. Chem. Soc. 120 (1998) 8340–8347.
[9] F.F. Alblewi, R.M. Okasha, A.A. Eskandrani, T.H. Afifi, H.M. Mohamed, A.H. Halawa, A.M. Fouda, A.-A.M. Al-Dies, A. Mora, A.M. El-Agrody, Design and synthesis of novel heterocyclic-based 4*H*-benzo[*h*]chromene moieties: targeting antitumor caspase 3/7 activities and cell cycle analysis, Molecules 24 (2019) 1060.
[10] H.E.A. Ahmed, M.A.A. El-Nassag, A.H. Hassan, H.M. Mohamed, A.H. Halawa, R.M. Okasha, S. Ihmaid, S.M. Abd El-Gilil, E.S.A.E.H. Khattab, A.M. Fouda, A.M. El-Agrody, A. Aljuhani, T.H. Afifi, Developing lipophilic aromatic halogenated fused systems with specific ring orientations, leading to potent anticancer analogs and targeting the c-Src Kinase enzyme, J. Mol. Struct. 1186 (2019) 212–223.
[11] F.F. Alblewi, R.M. Okasha, Z.M. Hritani, H.M. Mohamed, M.A. El-Nassag, A.H. Halawa, A. Mora, A.M. Fouda, M.A. Assiri, A.A.M. Al-Dies, T.H. Afifi, Antiproliferative effect, cell cycle arrest and apoptosis generation of novel synthesized anticancer heterocyclic derivatives based 4H-benzo[h]chromene, Bioorg. Chem. 87 (2019) 560–571, https://doi.org/10.1016/j.bioorg.2019.03.059.
[12] T.H. Afifi, R.M. Okasha, H.E.A. Ahmed, J. Ilaš, T. Saleh, A.S. Abd-El-Aziz, Structure-activity relationships and molecular docking studies of chromene and chromene based azo chromophores: a novel series of potent antimicrobial and anticancer agents, EXCLI J. 16 (2017) 868–902.
[13] R.M. Okasha, F.F. Alblewi, A. Naqvi, T.H. Afifi, A.M. Al-Dies, A.M. El-Agrody, Design of new benzo[h]chromene derivatives: antitumor activities and structure-activity relationships of the 2,3-positions and fused rings at the 2,3-positions, Molecules 22 (3) (2017) 479–496.
[14] H.K. Abd El-Mawgoud, H.A.M. Radwan, F. El-Mariah, A.M. El-Agrody, Synthesis, characterization, biological activity of novel 1*H*-benzo[*f*]- chromene and *1*2H-benz*o*[f]chromeno[2,*3*-d]pyrimidine derivatives, LDDD 15 (8) (2018) 857–865, https://doi.org/10.2174/1570180814666171027160854.
[15] G. Singh, A. Sharma, H. Kaur, M. Ishar, Chromanyl-isoxazolidines as antibacterial agents: synthesis, biological evaluation, quantitative structure activity relationship, and molecular docking studies, Chem. Biol. Drug. Des. 87 (2016) 213–223.
[16] C. Bingi, N.R. Emmadi, M. Chennapuram, Y. Poornachandra, C.G. Kumar, J.B. Nanubolu, K. Atmakur, One-pot catalyst free synthesis of novel kojic acid tagged 2-aryl/alkyl substituted-4*H*-chromenes and evaluation of their antimicrobial and anti-biofilm, Bioorg. Med. Chem. Lett. 25 (2015) 1915–1919.
[17] M. Costa, T.A. Dias, A. Brito, F. Proença, Biological importance of structurally diversified chromenes, Eur. J. Med. Chem. 123 (2016) 487–507.
[18] V.Y. Korotaev, V.Y. Sosnovskikh, A.Y. Barkov, Synthesis and properties of 3-nitro-2*H*- chromenes, Russ. Chem. Rev. 82 (2013) 1081–1116.
[19] S.A. Patil, R. Patil, L.M. Pfeffer, D.D. Miller, Chromenes: potential new chemotherapeutic agents for cancer, Future Med. Chem. 5 (2013) 1647–1660.
[20] W. Gregor, G. Grabner, C. Adelwohrer, T. Rosenau, L. Gille, Antioxidant properties of natural and synthetic chromanol derivatives: Study by fast kinetics and electron spin resonance spectroscopy, J. Org. Chem. 70 (2005) 3472–3482.
[21] N. Jain, J. Xu, R.M. Kanojia, F. Du, G. Jian-Zhong, E. Pacia, M. Lai, A. Musto, G. Allan, M. Reuman, X. Li, D. Hahn, M. Cousineau, S. Peng, D. Ritchie, R. Russell, S. Lundeen, Z. Sui, Identification and structure-activity relationships of chromene-derived selective estrogen receptor modulators for treatment of postmenopausal symptoms, J. Med. Chem. 52 (2009) 7544–7569.
[22] A. Foroumadi, S. Emami, M. Sorkhi, M. Nakhjiri, Z. Nazarian, S. Heydar, S. Ardestani, F. Poorrajab, A. Shafiee, Chromene-based synthetic chalcones as potent antileishmani-al agents: synthesis and biological activity, Chem. Biol. Drug. Des. 75 (2010) 590–596.
[23] S. Kasibhatla, H. Gourdeau, K. Meerovitch, J. Drewe, S. Reddy, L. Qiu, H. Zhang, F. Bergeron, D. Bouffard, Q. Yang, J. Herich, S. Lamothe, S.X. Cai, B. Tseng, Discovery and mechanism of action of a novel series of apoptosis inducers with potential vascular targeting activity, Mol. Cancer Ther. 3 (2004) 1365–1373.
[24] K.-S. Lee, L.-Y. Khil, S.-H. Chae, D. Kim, B.-H. Lee, G.-S. Hwang, C.-H. Moon, T.-S. Chang, C.-K. Moon, Effects of DK-002, a synthesized (6aS, cis)-9,10-Dimethoxy-7,11b-dihydro indeno[2,1-c]chromene-3,6a-diol, on platelet activity, Life Sci. 78 (2006) 1091–1097.
[25] A.L. Albiston, S. DiWakarla, R.N. Fernando, S.J. Mountford, H.R. Yeatman, B. Morgan, V. Pham, J.K. Holien, M.W. Parker, P.E. Thompson, Identification and development of specific inhibitors for insulin-regulated aminopeptidase as a new class of cognitive enhancers, Br. J. Pharmacol. 164 (2011) 37–47.
[26] C. Bruhlmann, F. Ooms, P. Carrupt, B. Testa, M. Catto, F. Leonetti, C. Altomare, A. Cartti, Coumarins derivatives as dual inhibitors of acetylcholinesterase and monoamine oxidase, J. Med. Chem. 44 (2001) 3195–3198.
[27] S.R. Kesten, T.G. Heffner, S.J. Johnson, T.A. Pugsley, J.L. Wright, D.L. Wise, Design, synthesis, and evaluation of chromen-2-ones as potent and selective human dopamine D4 antagonists, J. Med. Chem. 42 (1999) 3718–3725.
[28] S.F. Thakor, D.M. Patel, M.P. Patel, R.G. Patel, Synthesis and antibacterial activity of novel pyrazolo[3,4-b]quinoline based heterocyclic azo compounds and their dyeing performance, Saudi Pharm. J. 15 (2007) 48–54.
[29] P.K. Nikhil, M.P. Pratik, R. Manoj, Study on antibacterial activity for multidrug resistance stain by using phenyl pyrazolones substituted 3-amino-1*H*-pyrazolon [3,4-b]quinoline derivative in vitro condition, Int. J. Pharm. Tech. Res. 3 (2011) 540–544.
[30] A.M. Khedr, M. Gaber, E.H. Abd El-Zaher, Synthesis, Structural Characterization, and Antimicrobial Activities of Mn(II), Co(II), Ni(II), Cu(II) and Zn(II) Complexes of Triazole-based Azodyes, Chin. J. Chem. 29 (6) (2011) 1124–1132, https://doi.org/10.1002/cjoc.201190211.
[31] S. Ginni, R. Karnawat, I.K. Sharma, P.S. Verma, Synthesis, characterisation and antimicrobial screening of some azo compounds, Inter. J. Appl. Biology Pharm. Technol. 2 (2011) 332–336.
[32] C. Kanter, H. Akal, B. Kaya, F. Islamoglu, M. Turk, S. Sasmaz, Novel phthalocyanines containing resorcinol azo dyes; synthesis, determination of pKa values, antioxidant, antibacterial and anticancer activity, J. Organomet. Chem. 783 (2015) 28–39.
[33] A.H. Abadi, A.A. Eissa, G.S. Hassan, Synthesis of novel 1,3,4-trisubstituted pyrazole derivatives and their evaluation as antitumor and anti-angiogenic agents, Chem. Pharm. Bull. 51 (2003) 838–844.
[34] S. Shoaib Ahmad Shah, G. Rivera, M. Ashfaq, Recent Advances in Medicinal Chemistry of Sulfonamides. Rational Design as Anti-Tumoral, Anti-Bacterial and Anti-Inflammatory Agents, Mini Rev. Med. Chem. 13 (1) (2013) 70–86, https://doi.org/10.2174/138955713804484749.
[35] European committee for antimicrobial susceptibility testing (EUCAST) of the European society of clinical microbiology and infectious diseases (ESCMID),

Determination of minimum inhibitory concentrations (MICs) of antibacterial agents by agar dilution, Clin. Microbiol. Infect. 6 (2000) 509–515.
[36] National Committee for Clinical Laboratory Standards. Methods for Dilution Antimicrobial Susceptibility Tests for Bacteria That Grow Aerobically, 5th ed., National Committee for Clinical Laboratory Standards (NCCLS), Wayne, PA, USA, 2000, Approved Standard M7-A5.
[37] T. Mossman, Rapid colorimetric assay for cellular growth and survival: application to proliferation and cytotoxicity assays, J. Immunol. Methods 65 (1983) 55–63.
[38] A.U. Rahman, M.I. Choudhary, W.J. Thomsen, Bioassay Technique for Drug Development, Harwood Academic Publishers ISBN 0-203-34349-2, 2001.
[39] M.A. Bhat, M. Imran, S.A. Khan, N. Siddiqui, Biological activities of sulfonamides, Indian J. Pharm. Sci. 67 (2005) 151–159.
[40] O.A. Christian, M.R. Ghadiri, Discovery of potent and selective histone deacetylase inhibitors via focused combinatorial libraries of cyclic α3β-tetrapeptides, J Med Chem. 52 (2009) 7836–7846.
[41] S. Ihmaid, H.E.A. Ahmed, M.F. Zayed, The design and development of potent small molecules as anticancer agents targeting EGFR TK and tubulin polymerization, Int. J. Mol. Sci. 19 (2018) 408.
[42] R.B. Durairaj, Resorcinol: Chemistry, Technology and Applications, Springer-Verlag, Berlin Heidelberg, 2005.
[43] A. Jordan, J.A. Hadfield, N.J. Lawrence, A.T. McGown, Tubulin as a target for anticancer drugs: agents which interact with the mitotic spindle, Med. Res. Rev. 18 (1998) 259–296.
[44] G.M. Morris, D.S. Goodsell, R.S. Halliday, R. Huey, W.E. Hart, R.K. Belew, A.J. Olson, Automated docking using a Lamarckian genetic algorithm and an empirical binding free energy function, J. Comput. Chem. 19 (1998) 1639–1662.
[45] M. Molecular Operating Environment (MOE) Chemical Computing Group, Quebec, Canada, 2012, < https://www.chemcomp.com > (accessed on 30/02/2013).